PEOPLE'S DEMOCRATIC REPUBLIC OF ALGERIA

Ministry of Higher Education and Scientific Research

University of Amar Telidji - Laghouat

Faculty of Technology

Department of Electronics

MASTER THESIS

DOMAINE: Science & Technology

FIELD: Electronics

SPECIALTY: Instrumentation

Bendjedid Oumaima Arbia & Dhina Aya

Theme

Modelling and Control of a Solar Micro-Inverter

Jury members:

SEGHIER Tahar	Prof	UATL	President
BELKHIRI Mohammed	Prof	UATL	Examiner
AMEUR Khaled	MCB	UATL	Supervisor
BENMILOUD Mohammed	MCB	UATL	Co-Supervisor

2023 / 2024

Abstract

This project aims to design and control a Solar Micro-Inverter using classical PI and PID controllers. This type of inverter is used in low-power (less than 2 kilowatts) standalone photovoltaic systems.

The inverter structure is based on two stages: the first stage consists of a static DC-DC push-pull converter based on a High-Frequency transformer, which ensure a galvanic isolation between the input and output circuits. This feature is crucial for protection against hazards. Using a high-frequency transformer also reduces the weight and size of the overall inverter. The second stage consists of a DC-AC Full-Bridge Inverter that allows for the production of alternative voltage and current.

During this study, each stage is modeled and controlled separately, then the both of them are joined together and controlled. The system was tested under variations in both input and load conditions. The results obtained were highly satisfactory and demonstrate the effectiveness of the designed controllers.

Keywords: Solar microinverter, push-pull converter, full bridge inverter, Ziegler-Nichols, multistage inverter

ملخص

يهدف هذا المشروع إلى تصميم محول ساكن مجهري، مستمر ـ متناوب، والتحكم فيه باستعمال منظمات كلاسيكية من نوع تناسبي ـ تكاملي و تناسبي ـ تكاملي ـ تفاضلي. يستخدم هذا النمط من المحولات في الأنظمة الكهروضوئية ذات القدرة المنخفضة (أقل من ٢ كيلو واط) والمستقلة عن الشبكة الكهربائية.

بنية المحول قيد الدراسة تعتمد على تركيبتين: التركيبة الأولى مكونة من محول ساكن مستمرمستمر رافع للجهد يعتمد على محول عالي التردد ممّا يسمح بالعزل الكهربائي بين الدخل والخرج، وهذه خاصية فائقة الأهمية من حيث الحماية من الأخطار. كما يسمح استعمال المحول عالي التردد بتقليل وزن وحجم المحول ككل. والتركيبة الثانية مكونة من محول بجسر كامل مستمر ـ متناوب يسمح بإنتاج جهد وتيار متناوبين.

تمت خلال هذه الدراسة نمذجة وتصميم المتحكم (المنظم) لكل تركيبة على حدة، ثم دمجهما معا. تم اختبار النظام تحت تغيرات كل من الحمل وتوتر الدخل. النتائج المتحصل عليها جد مرضية وتعكس نجاعة المتحكمات المصممة.

Résumé

Ce projet vise à concevoir et contrôler un micro-onduleur solaire en utilisant des régulateurs classiques PI et PID. Ce type d'onduleur est utilisé dans les systèmes photovoltaïques autonomes de faible puissance (moins de 2 kilowatts).

La structure de l'onduleur en question est basée sur deux convertisseurs élémentaires: Le premier consiste en un convertisseur DC-DC push-pull basé sur un transformateur de haute fréquence, assurant une isolation galvanique entre les circuits d'entrée et de sortie. Cette fonctionnalité est cruciale pour la protection contre les risques. L'utilisation d'un transformateur haute fréquence permet également de réduire le poids et la taille du Micro-onduleur. Le deuxième convertisseur élémentaire, comprend un onduleur DC-AC à pont complet permettant la production de tension et de courant alternatifs.

Au cours de cette étude, chaque convertisseur élémentaire est modélisé et contrôlé séparément, puis les deux sont combinées et contrôlées ensemble. Le système a été testé sous des variations de la tension d'entrée et de la charge. Les résultats obtenus étaient très satisfaisants et démontrent l'éfficacité des régulateurs conçus.

اهداء

من قال أنا لها نالها، وأنا لها، وإن أبت، رغماً عنها أتيت بها. نلتها وعانقت اليوم مجداً عظيماً. فعلتها بعد أن كانت مستحيلة، كانت دروباً قاسية وطرقاً خسرت بها الكثير، ولكنني آ وصلت آ، ولله الحمد والشكر.

إليك يا الله أرفع شكري وامتناني على نعمك ورحمتك التي لا تُحصى، فالحمد لله الذي يحكم بالحق ويجزي كل نفس بما تسعى.

ولهذا أهدي ثمرة جهدي إلى:

أبي الحبيب ، صاحب السيرة العطرة والفكر المستنير، من كان لي خير دعم وسند. شكرًا لك يا أبي على تشجيعك المستمر، وتوجيهاتك السديدة، وقوتك التي استندت عليها في أصعب الأوقات. حفظك الله وأدامك بصحة وعافية.

أمي العزيزة ، مصدر الحنان والمحبة، التي وضعتني على طريق الحياة وسلحتني بالقيم والمبادئ. أهديكِ هذا النجاح يا أمي، وأشكركِ من أعماق قلبي على دعمكِ المستمر وتضحياتكِ العظيمة. حفظكِ الله ورعاكِ.

أخواتي الغاليات ، شموع دربي، اللاتي كنّ لي سنداً ودعماً في كل خطوة. شكرًا لكنّ على وقوفكنّ بجانبي، وتحفيزكنّ لي في كل لحظة. حفظكنّ الله وأدامكنّ نوراً في حياتي.

أخي العزيز ، رفيق دربي وسندي في الحياة، الذي كان دائمًا بجانبي وداعماً لي في مشواري الدراسي. شكرًا لك على دعمك المستمر، وتحفيزك الذي لم ينقطع. هذا الإنجاز أهديه لك، وأتمنى أن يكون فخراً لنا جميعاً.

روح أخي الطاهرة ، الذي كان لي سندًا وأخًا وداعمًا في مشواري الدراسي. أدعو الله أن

يتغمده بواسع رحمته ويسكنه فسيح جناته. غيابك كان صعبًا، لكن ذكراك تبقى نبراسًا يضيء لي الطريق. لا أنسى دعمك وتشجيعك، وهذا النجاح أهديه لروحك الغالية.

صديقتي الغالية أميمة ، رفيقة الدرب، التي كانت دائمًا بجانبي في السراء والضراء. شكرًا لكِ على دعمكِ المتواصل وصداقتكِ الوفية.

أساتذتي المشرفين ، م. بن ميلود و خ. عامر، اللذين لم يبخلا بمد العون والإرشاد. شكرًا على توجيهاتكم القيمة ودعمكم المستمر.

إلى كل الأساتذة الذين لم يقصروا معنا، وكل من وقف بجانبي وساهم في هذا النجاح.

إلى كل هؤلاء، أهدي هذا العمل، وأسأل الله تعالى أن يتقبله خالصًا لوجهه الكريم.

دهينة آية

جامعة عمار ثليجي، الأغواط

جوان ٢٠٢٤

اهداء

(وَآخِرُ دَعْوَاهُمْ أَنِ الْحَمْدُ لِلَه رَبِ الْعَالَمِينَ)

الحمد لله حبا و شكرا و امتنانا ، ماكنت لأفعل هذا لولا فضل الله فالحمد لله على البدء و الختام لم تكن الرحلة قصيرة و لا ينبغي لها أن تكون لم يكن الحلم قريبا و لا الطريق كان محفوفا بالتسهيلات لكنني فعلتها و نلتها

أهدي تخرجي الى تلك الانسانة العظيمة ، لطالما تمنيت ان تقر عينها برؤيتي في يوم كهذا الى التي توسدها التراب قبل أن تحقق أمنيتها ، الى سر مناضلتي واجتهادي فرحتي تنقصها وجودك و نجاحي ينقصه فخرك بي الى روح جدتي الطاهرة رحمك الله و جمعنا و اياك في دار الخلود يا رب

الى الذي زين اسمي بأجمل الألقاب ، من دعمني بلا حدود و أعطاني بلا مقابل الى من علمني أن الدنيا كفاح و سلاحها العلم و المعرفة ، الى من غرس في روحي مكارم الأخلاق داعمي الأول في مسيرتي و سندي و قوتي و ملاذي بعد الله ، الى فخري و اعتزازي **والدي**

الى من جعل الله الجنة تحت أقدامها و احتضنني قلبها قبل يدها و سهلت لي الشدائد بدعائها الى القلب الحنون و الشمعة التي كانت لي في الليالي المظلمات ، سر قوتي و نجاحي و مصباح دربي الى وهج حياتي **والدتي**

الى ضلعي الثابت و أمان أيامي الى ملهمي نجاحي الى من شددت عضدي بهم فكانوا لي ينابيع أرتوي منها الى خيرة أيامي و صفوتها الى قرة عيني **(أخي و أخواتي)**

الى رفيقة دربي و صديقتي آية الى من رافقتي في حزني و في فرحي و شاطرتني لحظات النجاح ، في غمضة عين مرت أيامنا ، و ها نحن اليوم نجني قطافنا ، و نودع المكان الذي ضمنا

بالأمس التقينا و اليوم نفترق و لكن فرحنا بتخرجنا ينسينا ألمنا

الى أساتذتي المشرفين من كانوا عونا و سندا في انجاز هذه المذكرة **الأستاذ م .بن ميلود** و **الأستاذ خ. عامر** شكرا على توجيهاتكم و دعمكم لنا جعله الله في ميزان حسناتكم ان شاء الله

لكل من كان عونا و سندا في هذا الطريق أخوالي و عائلتي ... لرفقاء السنين و أصحاب الشدائد و الأزمات الى من رسموا بسمتي وقت الصعاب و كل من كان له الأثر في انجازي أهديكم هذا الانجاز و ثمرة نجاحي الذي لطالما تمنيته ها أنا اليوم أتممت أول ثمراته

راجية من الله تعالى أن ينفعني بما علمني و أن يعلمني ما أجهل و يجعله حجة لي لا علي.

بن جديد أميمة العربية
جامعة عامر ثليجي، الأغواط
جوان ٢٠٢٤

Contents

List of Figures

General Introduction

Photovoltaic (PV) solar power systems are among the renewable energy systems that are now considered one of the best environmentally friendly renewable energy solutions for power generation in Algeria. It is proving to be a game changer, bringing sustainable solutions to various sectors such as agriculture, education, public infrastructure, and residential areas.

Power generation in PV systems relies on several essential components. Typically, a PV system includes PV panels that capture sunlight and convert it into direct current (DC) electricity. A solar controller manages the power flow and prevents overcharging the batteries, which store the energy for later use. An inverter then converts the stored DC electricity into alternating current (AC), which is the type of electricity used in most homes, agriculture and public infrastructures.

In this work, we study solar inverters, which are the most crucial and sensitive component of a PV system. Due to their constant operation and exposure to fluc-

Electrification by photovoltaic system of Aouissi Ali primary school,Laghouat.

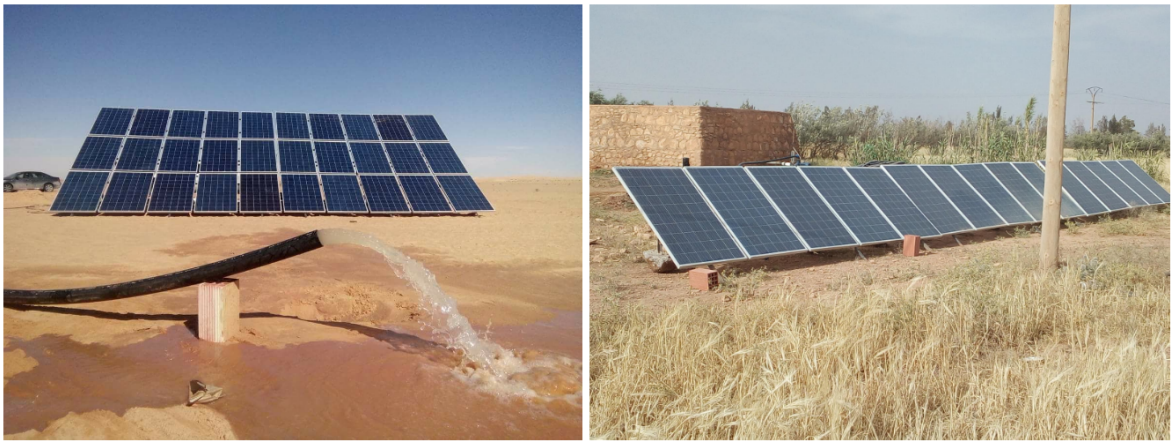

Solar irrigation by Mekk Energy, Sidi Makhlouf region, Laghouat.

tuating environmental conditions, inverters are prone to overheating and burnout, making their reliability and efficiency important for the overall performance of the solar power system.

One of the most commonly used solar inverter topologies is the multistage inverter, particularly the two-stage configuration, which is widely adopted. In this setup, the first stage involves a DC-DC converter that adapts the voltage from the PV panels, ensuring it is at an appropriate level for the next stage. The second stage is a DC-AC inverter that converts the adapted DC voltage into AC voltage, making it suitable for use in various applications.

This master's thesis focuses on improving the performance of micro-inverters by developing a control strategy for both the DC/DC and DC/AC stages. The DC/DC stage involves an isolated DC/DC converter, known as push-pull converter, while the DC/AC stage uses a full bridge inverter. This is accomplished by modeling the system using average state-space representation. The control scheme is developed using the Ziegler-Nichols approach to ensure the stabilization of the DC bus voltage and guarantee an accurate tracking of a sine wave reference for the AC voltage.

The master thesis will be structured into four chapters, with a general introduction and conclusion:

- **Chapter 1:** This chapter provides an overview of photovoltaic solar power systems, focusing on power converters and distinguishing between isolated and non-isolated DC-DC converter topologies. It emphasizes the importance

Electrification by photovoltaic system of Off-grid homes (for lighting, appliances, etc)

of implementing a two-stage micro-inverter topology.

- **Chapter 2:** This chapter explores the modeling and control of the push-pull converter using state-space representation and PI controller design.
- **Chapter 3:** Chapter Three delves into the operational principles of the Full-Bridge converter, providing its mathematical model and introduces a PI controller designed to regulate its output voltage.
- **Chapter 4:** This chapter integrates both stages DC/DC and DC/AC to achieve the stabilization of the DC bus voltage and achieve a good tracking of a sine wave reference of the AC output voltage.

These chapters lead to a general conclusion and future works of this project.

1 Overview of PV Systems and Power Conversion Technologies

1.1 Introduction

This chapter provides a comprehensive overview of photovoltaic systems and their essential components, with a particular emphasis on micro-inverters. It explains the structures that constitute micro-inverters, such as DC-DC converters, and covers both isolated and non-isolated converters, as well as DC-AC converters. Furthermore, this chapter presents an in-depth exploration of the topology chosen for this project.

1.2 Photovoltaic System and its main components

A photovoltaic (PV) system refers to a setup that uses solar panels to convert sunlight directly into electricity. It is considered environmentally friendly solution because it reduces carbon emissions and decreases reliance on fossil fuels, thereby contributing to mitigating climate change. This system is employed in a wide range of applications, from home lighting to powering devices in rural health centers, as well as public lighting in remote areas.

Solar panels are composed of photovoltaic cells, which are the fundamental components made from semiconductor materials, typically silicon, that generate an electric current when exposed to light. Solar panels are mounted on rooftops or on the ground to capture sunlight.

Figure 1.1 shows the main components of a standalone PV system, commonly used in remote areas or off-grid applications. Typically, it includes solar panels, a solar controller, a storage battery, an inverter, and a load. The following subsections will discuss each component in detail.

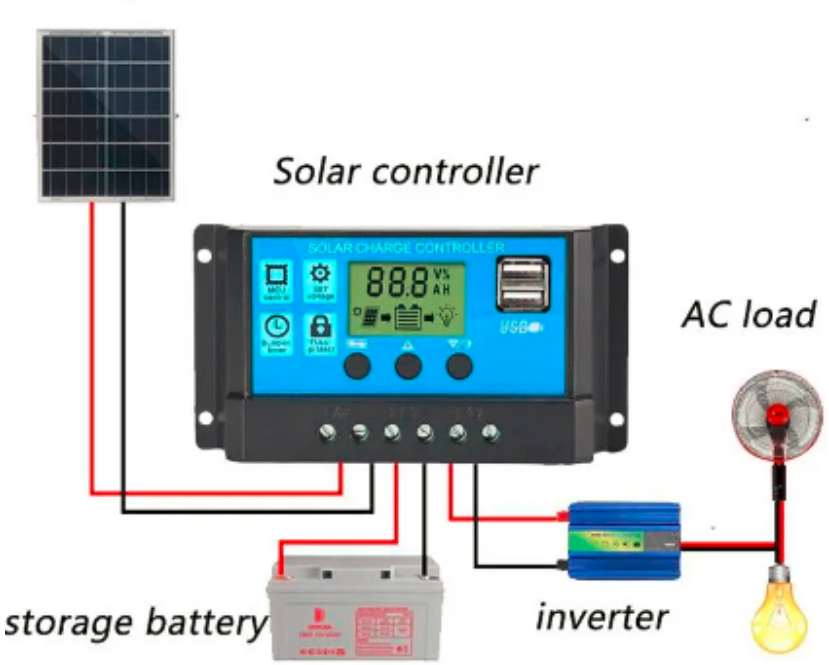

Figure 1.1: Main parts of a standalone PV system.

1.2.1 Solar panels

Solar panels, consist of multiple silicon solar cells that transform sunlight into electricity, see Figure 1.2. Encased between a glass front sheet and a polymer back sheet, they are secured within an aluminum frame. Typically, these panels are pre-assembled with cables for easy connection to each other and to an inverter [1].

1.2.2 Solar inverters

Inverters are used to convert the direct current (DC) generated by the solar panels into alternating current (AC), typically used in residential settings. There are many inverter technologies to choose from:

Figure 1.2: Solar panels

Centralised inverter

Centralized inverters are typically employed in extensive power plants benefiting from consistent sunlight exposure, such as desert-based power stations, ground-based power stations, and other large-scale power generation systems. These systems typically operate at high power capacities, commonly exceeding megawatt levels [2].

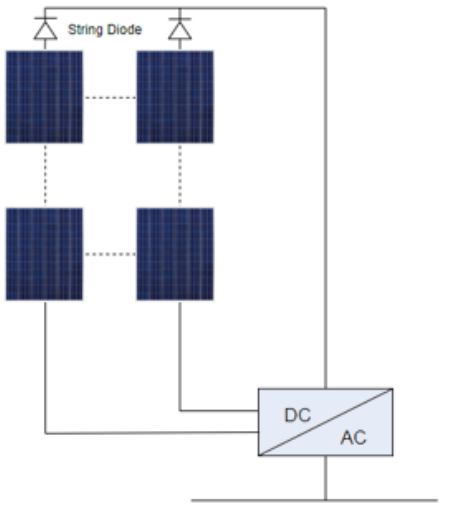

Figure 1.3: Centralised inverter

String inverter

In string inverter setups, solar panels are arranged in series to form strings, which are then connected in parallel to each inverter, creating an array. String inverters are usually cost-effective, requiring only one device for multiple panels, and are efficient at converting DC to AC power. However, they have a drawback: if one panel in a string is shaded or produces less due to dirt or other factors, it reduces the output of all panels in that string [2, 3].

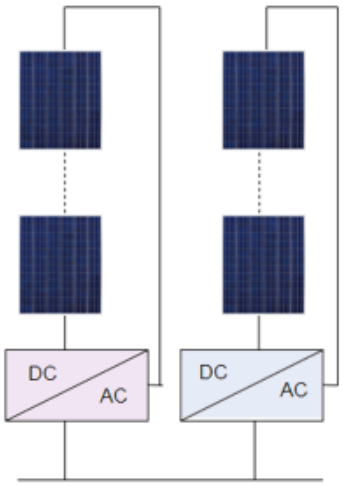

Figure 1.4: String inverter

Multi-string inverter

In this case, certain strings are connected to their own DC converter, which is then connected to the AC inverter. Each string can be independently regulated, resulting in increased efficiency within this framework [2, 3, 4].

Micro inverter (AC module)

Micro-inverters are similar to DC-to-DC converters in that they optimize the output of solar panels at the panel level. The difference is that they also perform the DC to AC conversion so that no string inverter is required at all. Micro-inverters may be mounted externally to the solar panel, or even come integrated into the module

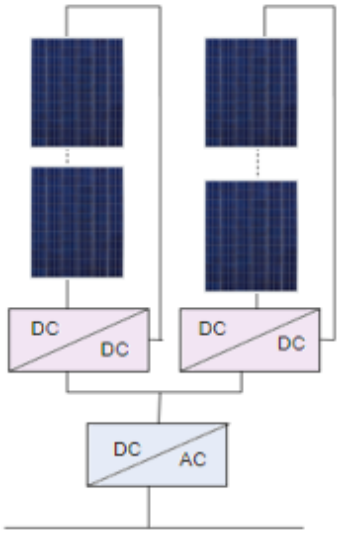

Figure 1.5: Multi-string inverter

in what is called an AC module. Using micro-inverters can greatly reduce the complexity of the system and therefore the installation costs [4].

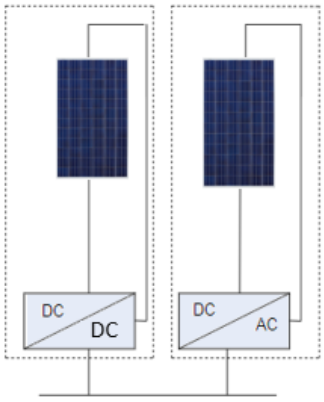

Figure 1.6: Micro inverter

1.2.3 Batteries

Incorporating batteries into a solar PV system enables the storage of energy generated by the solar panels for use during periods when sunlight is not available, such as at night. They are typically essential components in off-grid systems. Figure 1.7 shows a 12V 100AH lead acid battery used in PV systems.

Figure 1.7: Example of a solar battery 12V, 100AH.

1.2.4 Solar Charge Controller

Charge controllers, Figure 1.8, are necessary when integrating batteries into your system, and when not using a hybrid inverter. They regulate the flow of power to the batteries, safeguarding against overnight discharges via the solar panels, and offer monitoring capabilities for both the batteries and solar panels [5].

Figure 1.8: Example of a charge controller.

1.3 Micro-Inverters

A micro-inverter is a small device in solar PV systems that converts DC output from a single solar module into AC, suitable for home electrical systems or the grid. Micro-inverters have some advantages, like tracking real-time solar intensity, monitoring, reliability, improved safety, and longer warranties. They have two main designs:

1.3.1 Single-Stage Micro-Inverter

The applied DC voltage is converted to a 50 Hz AC voltage using one of DC-AC converters, which is then fed into the public grid, as shown in Figure 1.13. Its benefits include high reliability due to fewer components and safety through galvanic isolation of the DC and AC sides. However, it suffers from low efficiency due to high transformer losses, and it is heavy and bulky primarily because of the 50 Hz transformer.

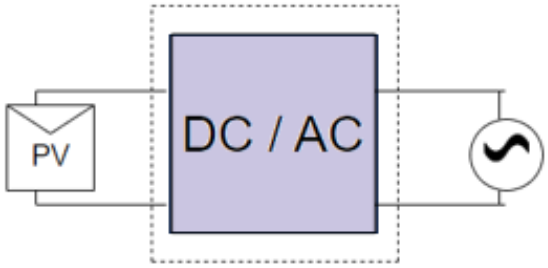

Figure 1.9: The diagram of Single-Stage.

1.3.2 Multi-stage Micro-Inverter

In multi-stage systems, direct current (DC) is converted to alternating current (AC) through two stages. The first stage relies on the push-pull transformer, which generates a high-frequency square wave signal ranging from 20 kHz. The bridge rectifiers convert the square wave signal back into DC voltage and store it in the intermediate circuit. Then, a second stage relies on full bridge generates a 50 Hz square wave AC voltage, which is smoothed to a sinusoidal AC voltage at 50 Hz before being fed into the public grid. Its benefits include compactness and lightweight due to its small and lightweight design, high efficiency through reducing transformer losses, safety through galvanic isolation between the DC and AC sides.

In the next subsection, we will consider each part of a multistage inverter in detail, as these components play a fundamental role in the development of the micro-inverter.

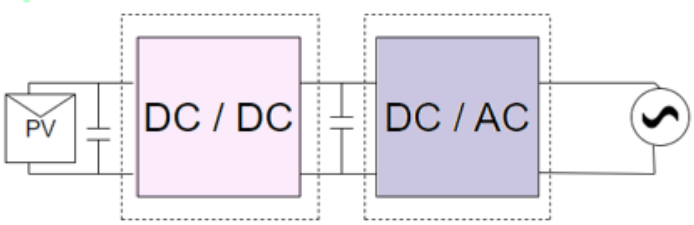

Figure 1.10: The diagram of Multi-Stage.

DC-DC Converter

DC-DC converters are electronic devices designed to efficiently convert one DC voltage to another. They are widely used to transform and distribute DC power in various systems and instruments. DC/DC converters are classified according to their topology, mode of operation, and output voltage regulation. The topology determines the switching method used to control the voltage level. The mode of operation explains how the converter functions during the switching process. Output voltage regulation refers to the method used to manage the converter's output voltage. The main types of DC/DC converters are the Buck Converter, Boost Converter, Buck-Boost Converter, Flyback Converter, Forward Converter, and push-pull Converter.

- Non-Isolated Converter:

Non-isolated converters lack magnetic and electrical isolation between the input and output circuits because they do not include a transformer. The input and output share the same ground reference and have a direct electrical connection between them. Compared to isolated converters, non-isolated converters are a simpler and less expensive option. They are widely used in applications that do not require isolation or when the input and output share the same ground reference.

- The main types of non-isolated converters are the buck converter, boost converter, and buck-boost converter.

- Isolated Converter:

Isolated converters provide electrical isolation between the input and output circuits, typically using transformers or optocouplers. The primary advantage of

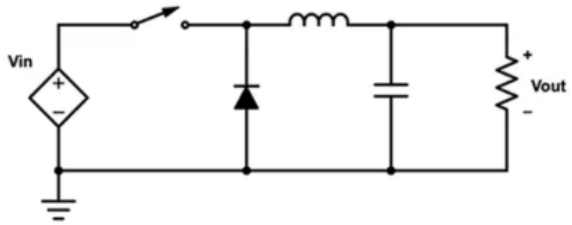

Figure 1.11: Non-isolated circuit diagram.

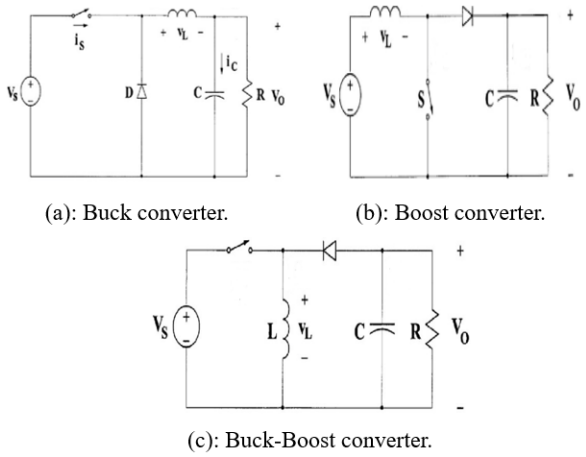

Figure 1.12: The circuits types of Non-Isolated converter .

these converters is their ability to offer galvanic isolation, meaning there is no direct electrical connection between the input and output. This isolation provides several benefits, including enhanced safety, noise reduction, the capability to handle voltage differences, and the elimination of ground loops. Isolated converters are commonly used in applications where safety and isolation are crucial, such as in medical equipment, industrial controls, power supplies, and communication systems.

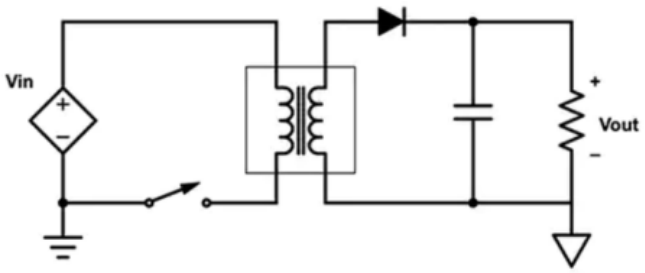

Figure 1.13: Isolated circuit diagram.

- The main type of Isolated converter are the fly-back converter, forward con-

verter, push-pull converter, and full-bridge converter.

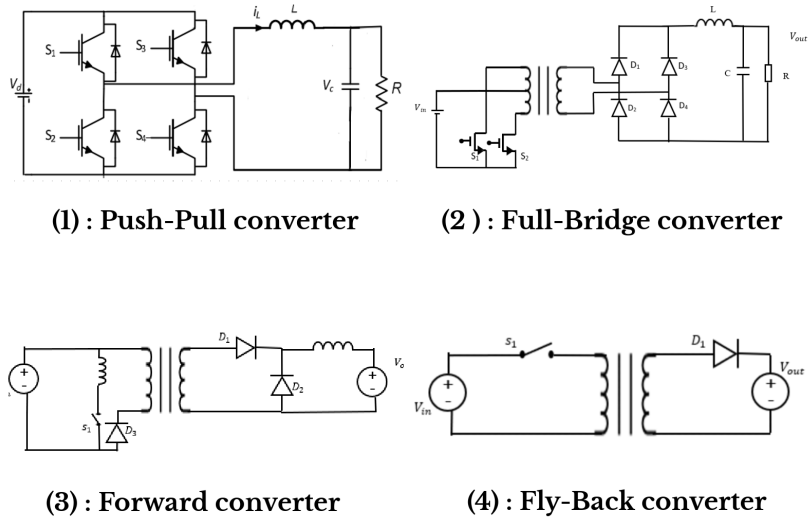

Figure 1.14: The circuits types of Isolated converter.

DC-AC Converter

The single phase full bridge inverter converts DC (direct current) to AC (alternating current) using a configuration that includes four switches arranged in a bridge layout. Typically, two switches are connected to each DC voltage source (positive and negative) and two to the load. These switches, often semiconductor devices like MOSFETs or IGBTs, alter the output voltage polarity through their switching sequence to generate an AC voltage. Voltage output can be adjusted by changing the switching pattern and DC input voltage. The output waveform can resemble either a pure sine wave or a modified sine wave, depending on the switching strategy used, with frequency determined by the inverter's switching frequency. It offers high efficiency and adaptability to diverse loads and voltage levels, though its complexity and cost necessitate expertise in power electronics and control systems for optimal design and operation.

Transformer

In general, a transformer can be described as a device that increases or decreases voltage. The choice of a suitable transformer depends on certain characteristics, such as power, voltage level, frequency, and power factor, which in turn determine the transformer's size, type, and isolation class.

Figure 1.15: Example of transformer Ferrite-based.

Rectifier:

In electronics, rectifier circuits are the most commonly used because nearly all electronic devices operate on DC. Therefore, diodes are utilized in specific types of DC-DC converters for rectification, enabling current to flow in one direction and preventing reverse flow.where we find them in two basic forms:

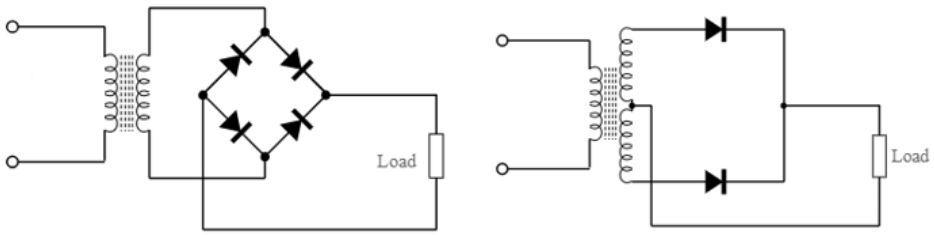

Figure 1.16: Basic Forms of Rectifier.

At this level, we have highlighted the main parts of a multistage inverter. In this master project, we will study a multistage inverter where the DC/DC stage

consists of a push pull converter and the DC/AC stage consists of a full bridge inverter. The main objective is to enhance the performance of the microinverter through the control of the two stages.

1.4 Conclusion

In this chapter, we have provided a comprehensive overview of photovoltaic systems and their essential components, with a particular emphasis on micro-inverters. We have explained the structures that constitute micro-inverters, such as DC-DC converters, covering both isolated and non-isolated types, as well as DC-AC converters. Furthermore, we highlighted the chosen topology for this project. In the following chapter, we will consider the first stage (push-pull converter) of the microinverter, from modelling to control design.

2 Modelling & Control of Push-Pull Converter

2.1 Introduction

In this chapter, we present a comprehensive understanding of the Push-Pull converter and its operating principle, detailing its mathematical model for simulation and control using a PI controller. This controller ensures the stabilization of the output voltage around a specified reference voltage with no steady-state error despite variations in load and input voltages.

2.2 The Push-Pull Converter Topology

The push-pull converter is one of the most important isolated converters due to its numerous advantages. It is efficient in energy utilization thanks to its topology, which efficiently utilizes the core. Additionally, it can be designed in smaller sizes compared to some other topologies. Its bidirectional operation capability (efficient operation in both directions) contributes to system cost reduction and noise reduction [6].

The basic structure of a Push-pull converter is shown in Figure 2.1. The push-pull converter includes a transformer, two switches (IGBT), and two diodes with filter (LC). The transformer, which is crucial for voltage conversion and isolation, typically features a center-tapped primary winding and two secondary windings.

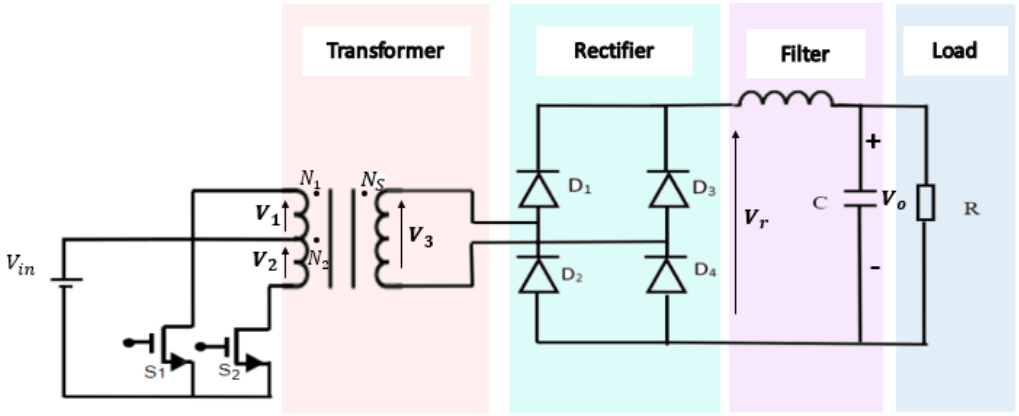

Figure 2.1: The circuit of Push-Pull Converter.

2.3 Operation Modes of Push-Pull Converter

2.3.1 Mode 1: Conduction of S_2 with S_1 Off

This mode corresponds to the state where S_2 is on and S_1 is off, as shown in the Figure 2.2 . In this case, the input voltage, denoted by V_{in}, is applied across half of the primary winding of the transformer (V_1) [7] .

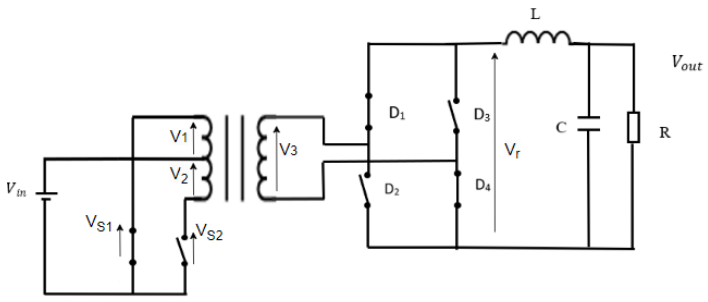

Figure 2.2: Equivalent circuit of Mode 1.

All the dotted ends of the transformer windings are now positive. Hence, the voltage on the secondary side, denoted by V_3, is positive and is measured by the transformer turns ratio (N_s/N_p) [7] :

$$V_3 = \frac{N_s}{N_p} V_{in} \tag{2.1}$$

Where N_1 = N_2= N_p and N_3 = N_s correspond to the primary and secondary windings of the transformer, respectively.

The diodes D_1 and D_4 are forward-biased while D_2 and D_3 are reverse-biased. This means that the voltage at the filter input, denoted by V_r, is equal to V_3. Considering this, the dynamics of the inductor current can be obtained by applying Kirchhoff's Voltage Law [7], which results in:

$$L\frac{di_L(t)}{dt} = V_r - V_o \tag{2.2}$$

In the same manner and using Kirchhoff's Current Law, one can derive the dynamic equation for the voltage across the capacitor, denoted as V_o:

$$C\frac{dV_o(t)}{dt} = i_L(t) - \frac{1}{R}V_o(t) \tag{2.3}$$

Where L and C refer to the inductance and capacitance of the LC filter, and R represents the load resistance. From (2.2) and (3.3), the dynamics of mode 1 are given by:

$$\dot{x}(t) = A_1 x(t) + B_1 \tag{2.4}$$

Where the state variables $x(t) = [i_L(t) \quad V_o(t)]^T$ are the inductor current and the capacitor voltage. The state and input matrices for this mode (A_1 and B_1) are as follows:

$$A_1 = \begin{bmatrix} 0 & -\frac{1}{L} \\ \frac{1}{C} & -\frac{1}{RC} \end{bmatrix}, B_1 = \begin{bmatrix} \frac{N_s}{N_P}\frac{V_{in}}{L} \\ 0 \end{bmatrix} \tag{2.5}$$

2.3.2 Mode 2: Conduction of S_1 with S_2 Off

This mode corresponds to the state where S_2 is off and S_1 is on, as shows in Figure 2.3. In this case, the input voltage is applied across the second half of the primary winding (V_2)[7].

All the dotted ends of the transformer windings are now negative. Consequently, the voltage on the secondary side, V_3, becomes negative:

$$V_3 = -\frac{N_s}{N_p}V_{in} \tag{2.6}$$

Therefore, the diodes D_1 and D_4 are reverse-biased, while D_2 and D_3 are forward-biased. In this case, the filter input voltage is a rectified form of V_3:

$$V_r = \frac{N_s}{N_p}V_{in} \tag{2.7}$$

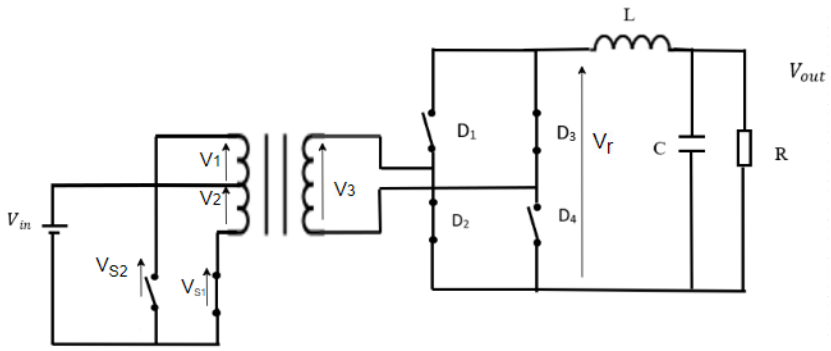

Figure 2.3: Equivalent circuit When S_1 is OFF and S_2 is ON,

Consequently, the dynamics of mode 2 are similar to the dynamics of mode 1 given by (2.4). We have:

$$\dot{x}(t) = A_2 x(t) + B_2 \tag{2.8}$$

where $A_2 = A_1$ and $B_2 = B_1$.

2.3.3 Mode 3: Conduction of S_1 with S_2 Off

This case corresponds to the state where S_2 and S_1 are both off, as shows in Figure 2.4. Under these conditions, no voltage is applied across the transformer windings, and the inductor current continues to flow through the freewheeling diodes (D_1-D_4 and D_2-D_3). The dynamics of mode 3 are given by (2.2) and (3.3) for $V_r = 0$ [7]. One can get:

$$\dot{x}(t) = A_3 x(t) + B_3 \tag{2.9}$$

where $A_3 = A_1$ and $B_3 = 0_{21}$ is a zero matrix with two rows and one column.

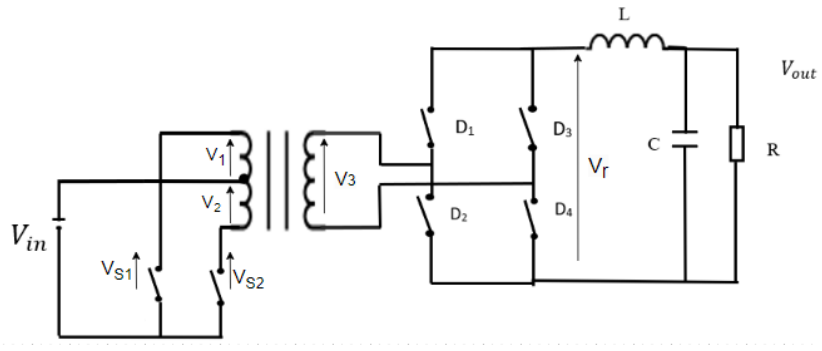

Figure 2.4: Equivalent circuit When S_1 is OFF and S_2 is OFF.

2.4 Average model of a push-pull converter

2.4.1 State-Space Representation

Figure 2.5 illustrates the wave-forms of the push-pull converter, including the switching signals (S_1 and S_2), the transformer output voltage V_3, and the rectified voltage V_r. This scenario is obtained by considering control signals with the same duty cycle (d) and a phase shift of 180 degrees. The duty cycle d corresponds to the average value of the control signal (S_1 or S_2) during the switching period T. To prevent mode 4, where both switches are on, the duty cycle d must remain less than 0.5[7].

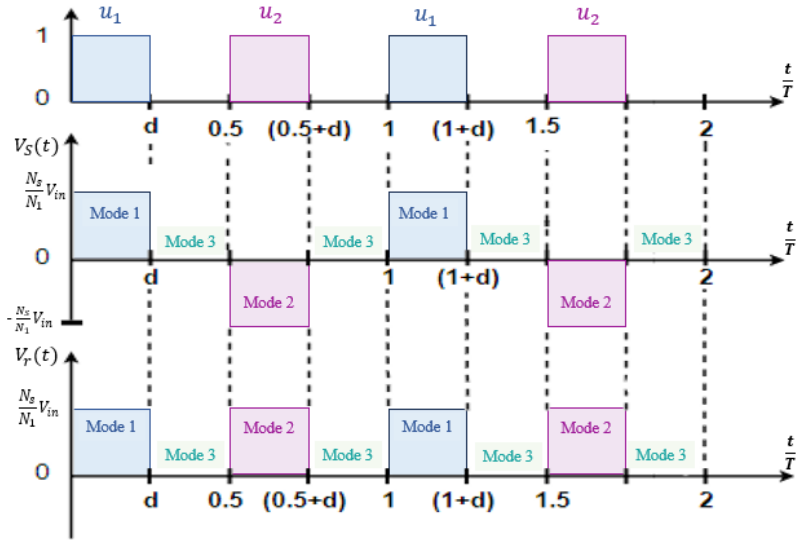

Figure 2.5: Output voltage of The transformer (V_3) and the rectified voltage (V_r) of the push-pull converter.

For any value of d less than 0.5, we get the same sequence of modes: mode 1, mode 3, mode 2, and then mode 3. Therefore, during a single switching period T, the average model of the converter can be written as follows:

$$\dot{X}(t) = \mathbf{A}X(t) + \mathbf{B}U(t) \tag{2.10}$$

where $X(t)$ is the average value of $x(t)$ over T, $U(t)$ corresponds to the duty cycle

d, the state and input matrices are given by [7]:

$$\begin{aligned} \mathbf{A} &= A_1 d + 2A_3(0.5 - d) + A_2 d = A_1 \\ \mathbf{B}U(t) &= B_1 d + 2B_3(0.5 - d) + B_2 d = 2B_1 d \end{aligned} \tag{2.11}$$

$$\mathbf{A} = A_1 = \begin{bmatrix} 0 & -\frac{1}{L} \\ \frac{1}{C} & -\frac{1}{RC} \end{bmatrix}, \mathbf{B} = 2B_1 = \begin{bmatrix} \frac{2N_s}{N_p L} V_{in} \\ 0 \end{bmatrix} \tag{2.12}$$

2.4.2 Transfer Function

The output of the system corresponds to the output voltage V_o. The transfer function of the system model can be calculated by:

$$G(s) = \frac{Y(s)}{U(s)} = C\varphi(s)B + D \tag{2.13}$$

with

$$\varphi(s) = [sI - A]^{-1}, \quad C = [0 \quad 1], \quad D = 0 \tag{2.14}$$

This yields to the following transfer function of the converter:

$$G(s) = \frac{2\frac{N_s}{N_p} V_{in}}{LCs^2 + \frac{L}{R}s + 1} \tag{2.15}$$

For our work, we used the parameters reported in Table 2.1 for control design as well as for simulations. These parameters are obtained from an experimental setup at LACoSERE laboratory which corresponds to 1.6KW solar microinverter.

Parameters	**Values**
Input voltage V_{in}	24v
inductance (L)	1.57 mH
capacitor (C)	340 μF
Load resistance (R)	217 Ω
Output Fundamental frequency	20KHz

Table 2.1: The parameters of Push-Pull converter.

For more general case of parameters design, one can refer to Table 2.2. The current ΔI and voltage ripple ΔV are given by the following expressions

$$\Delta I = \frac{Vin \times \Delta T}{2 \times L \times f} \tag{2.16}$$

Component/parameter	Formula
Input power	$P_{\text{in}} = \frac{P_{\text{out}}}{0.9}$
Maximum average input current	$I_{\text{in}} = \frac{P_{\text{in}}}{V_{\text{in}}}$
Transformer turns ratio	$N = \frac{V_{\text{out}}}{2 \times D_{\text{min}} X V_{\text{in}}}$
Maximum average output current	$I_{\text{out}} = \frac{P_{\text{out}}}{V_{\text{out}}}$
Filter inductor value	$L \geq \left(\frac{N_2}{N_1} V_{\text{in}} - V_{\text{out}}\right) \frac{t_{\text{on}}}{\Delta I}$
Output filter capacitor	$C = \frac{1}{8} \frac{\Delta I}{\Delta V} T$

Table 2.2: Component/parameter values

$$\Delta V = \frac{\Delta IL \times (D \times Ton) \times (1 - D)}{2 \times C} \tag{2.17}$$

In the next section, we will present the proposed control scheme.

2.5 Proposed Control Strategy

2.5.1 Control Objectives

In multi-stage configurations of solar micro-inverters, the output voltage from the push-pull converter acts as the input voltage for a single-phase inverter. It is crucial to maintain this input voltage at a constant level to ensure the inverter operates reliably, efficiently, and with minimal harmonic distortion. Our goal is to achieve this by regulating the output voltage V_o(t) of the push-pull converter around a specified reference voltage, regardless of changes in load or input voltage[7].

2.5.2 Control Scheme

In our project, we will employ a PI controller and design it using the Ziegler-Nichols method to regulate the output voltage of the converter. Figure 2.6 shows the proposed control scheme.

In Ziegler-Nichols method, we set the parameters K_p and K_i based on a detailed analysis of the system response, these parameters are adjusted to achieve the desired performance [8]. Based on this method, the PI parameters are obtained by following these steps:

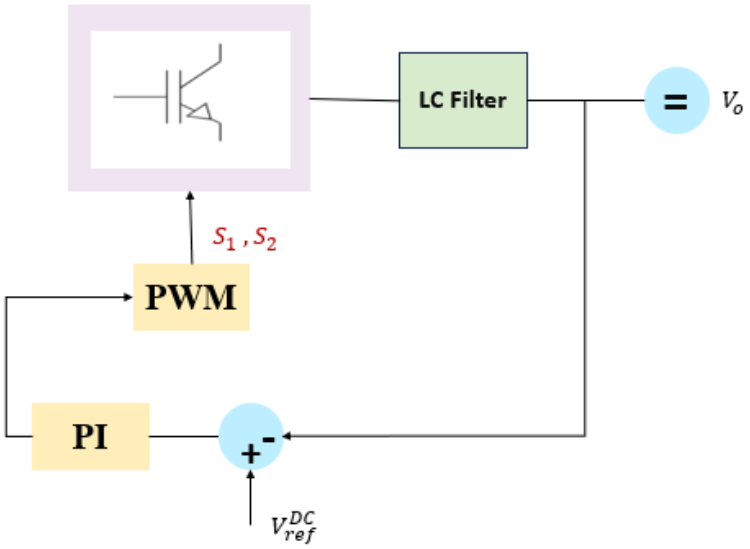

Figure 2.6: Control block diagram of a push-pull converter.

- We apply the correction constant to the system for closed-loop control.
- We apply a unit step input to the system with varying the value of k until the output reaches a pure sinusoidal waveform.
- Renaming k to k_u in order to give an oscillatory response.
- Tu : The cycle period as shows in figure 2.7 .

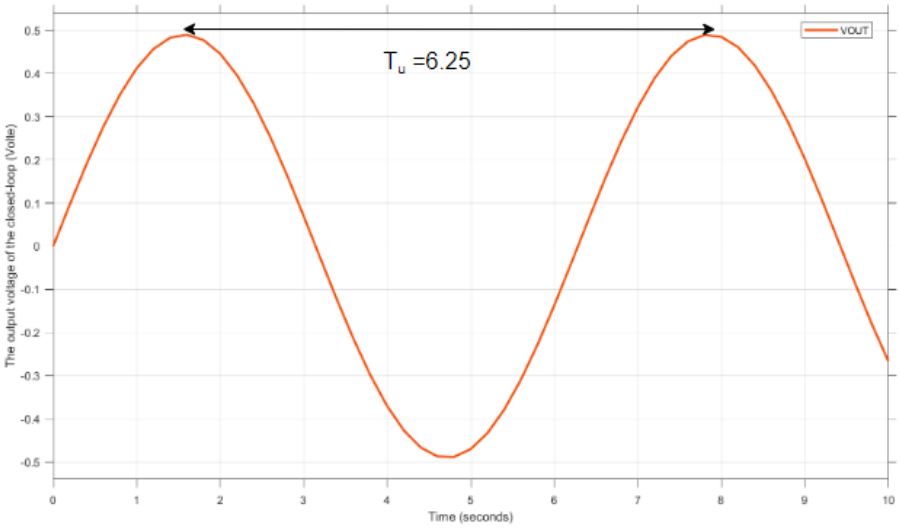

Figure 2.7: The output voltage of the close loop .

After these steps, the relations shown in the following table are applied to calculate the parameters of the PI controller. This yields to the following controller

Type of Controller	Controller C(s)	K_p	K_i
PI	$C(s) = K_p + \frac{K_i}{s}$	$0.45K_u$	$K_i = 0.54\frac{K_u}{T_u}$

Table 2.3: The parameters of PI controller .

parameters: $K_p = 0.432$; $K_i = 0.086$.

2.6 Simulation Results and Analysis

The aim of this part is to implement the proposed controller as well as the push-pull converter in Simulink/Matlab to test the closed loop system performance. To this end, we distinguish two cases, open loop and closed loop simulations.

2.6.1 Open-Loop Simulation

Figure 2.8 illustrates the implemented push-pull converter using SimScape blocks.

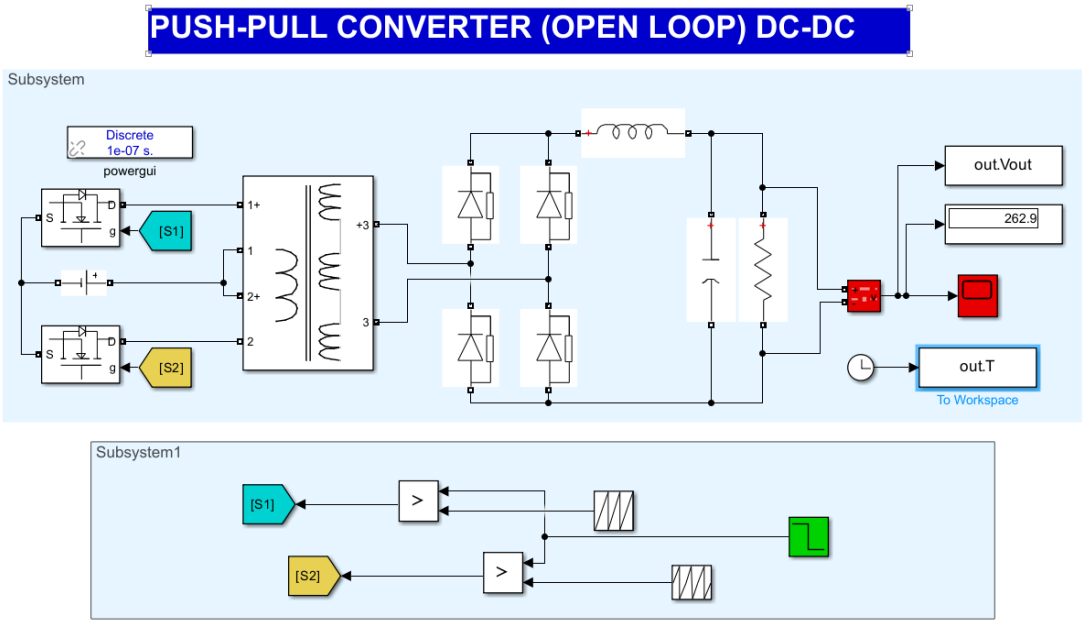

Figure 2.8: Open loop simulation of a push-pull converter with PWM generator.

Figure 2.9 represents the output of the transformer, which in turn represents the input of the rectifier. We remark three output voltage levels, which corresponds to the three operating modes of the converter:

$$\begin{cases} V_{out}^{transformer} = \frac{N_s}{N_p} V_{in} \\ V_{out}^{transformer} = 0 \\ V_{out}^{transformer} = -\frac{N_s}{N_p} V_{in} \end{cases} \tag{2.18}$$

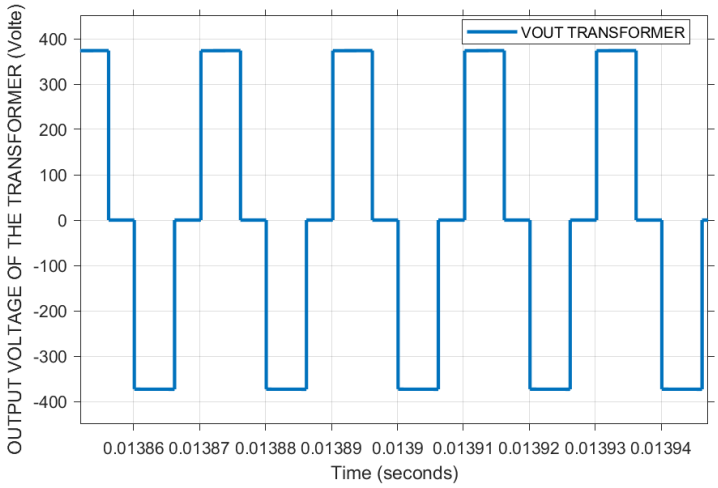

Figure 2.9: The output voltage of the transformer.

Figure 2.10 shows output of the rectifier, which in turn is the same output of transformer but it inverts the negative voltage to positive.

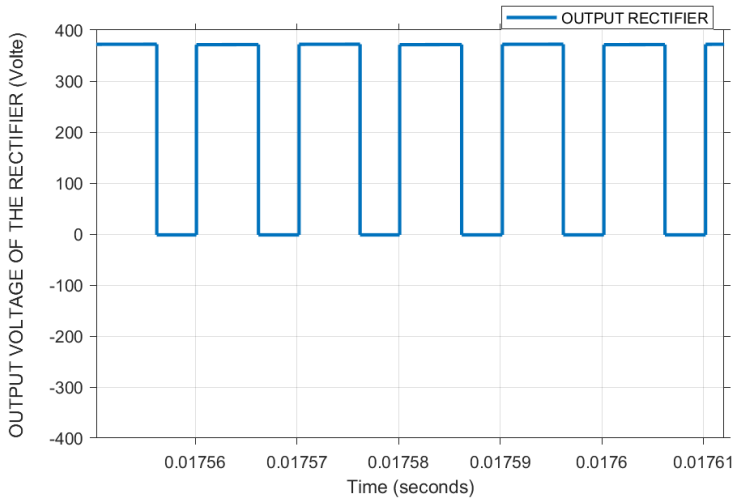

Figure 2.10: The output voltage of the Rectifier.

Figure 2.11 and Figure 2.12 represent the output voltage and current of the push-pull converter.

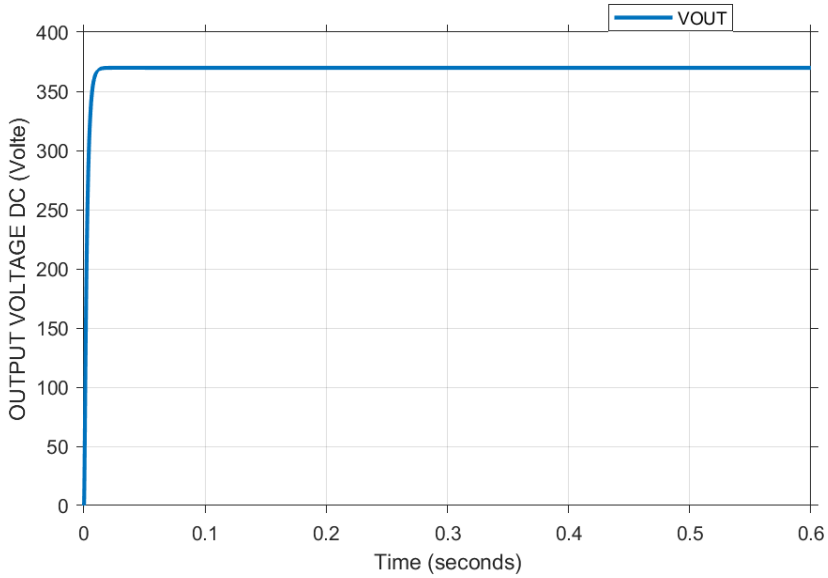

Figure 2.11: The output voltage of a push-pull converter for a duty cycle D=0.5.

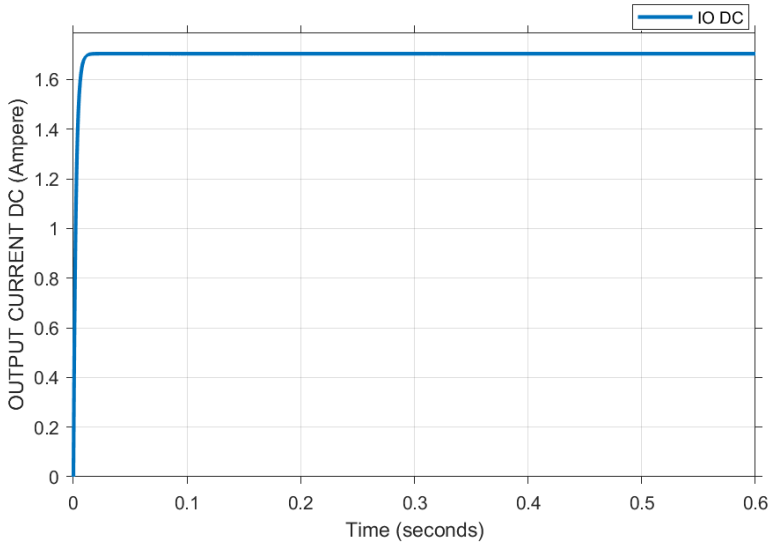

Figure 2.12: The output current I_L .

Variable Input Voltage

In this section, we made changes to the input V_{in} to observe the output voltage results. These changes involve setting the input voltage V_{in} to 24V initially, as shown in Figure 2.13. Subsequently, we adjusted the input voltage to 23V and then to 22V. Figure 2.14 illustrates the results obtained, clearly demonstrating that the open-loop system exhibits sensitivity to fluctuations in the input voltage.

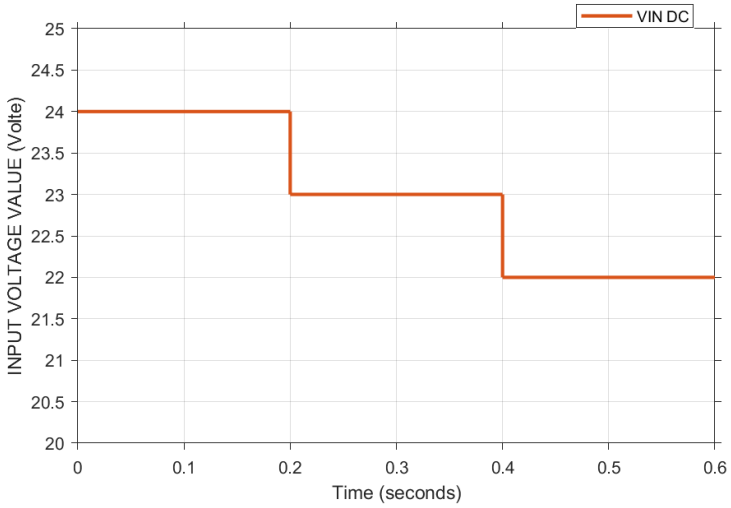

Figure 2.13: The input voltage variations.

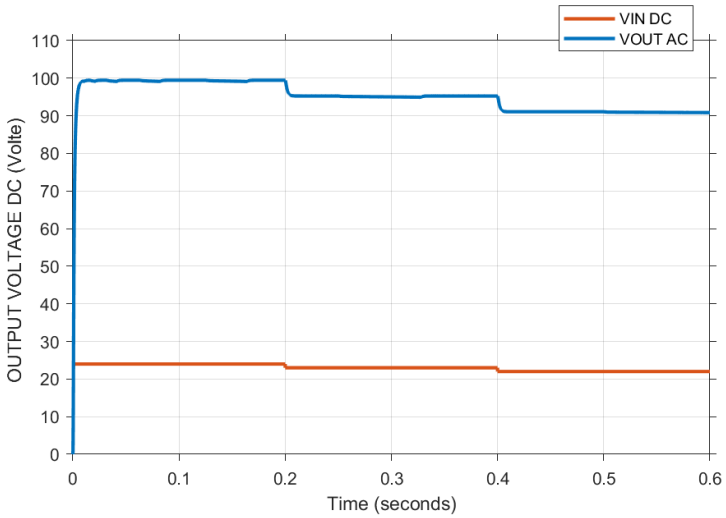

Figure 2.14: The output voltage of the push-pull converter under input voltage variations.

2.6.2 Variable Load

We changed R_{LOAD}, reducing its value from 400 ohms to 217 ohms, then returning it to its original value. The following figure illustrates the output voltage with the impact of these changes.

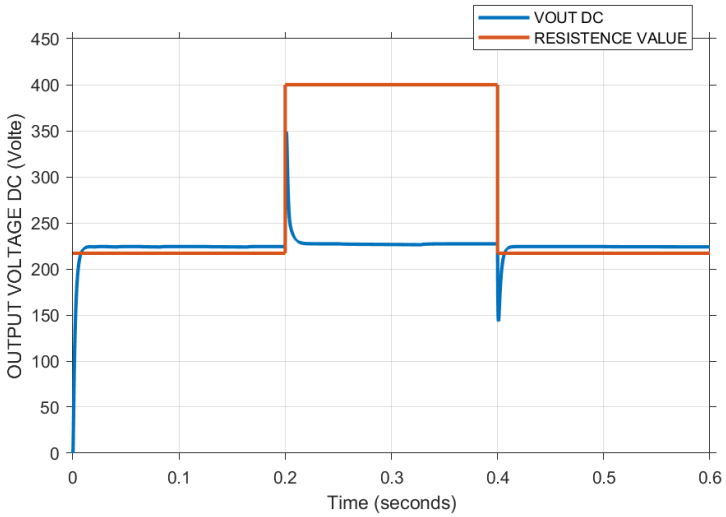

Figure 2.15: The output voltage under variable load.

The next section is devoted to the closed loop system under the proposed control strategy.

2.6.3 Closed-Loop Simulation

Figure 2.16 presents the simulink model of the push-pull converter in closed-loop. Three tests are considered, which corresponds to variable reference voltage, variable input voltage, and variable load.

Variable reference voltage

In this test, we conducted an experiment with a variable reference voltage. We adjusted the reference voltage every 0.2 seconds: first to 290 volts, then to 320 volts, and finally to 360 volts. The controller demonstrated a quick and effective response, ensuring that the output voltage followed the reference with zero steady-state error, as shown in Figure 2.17.

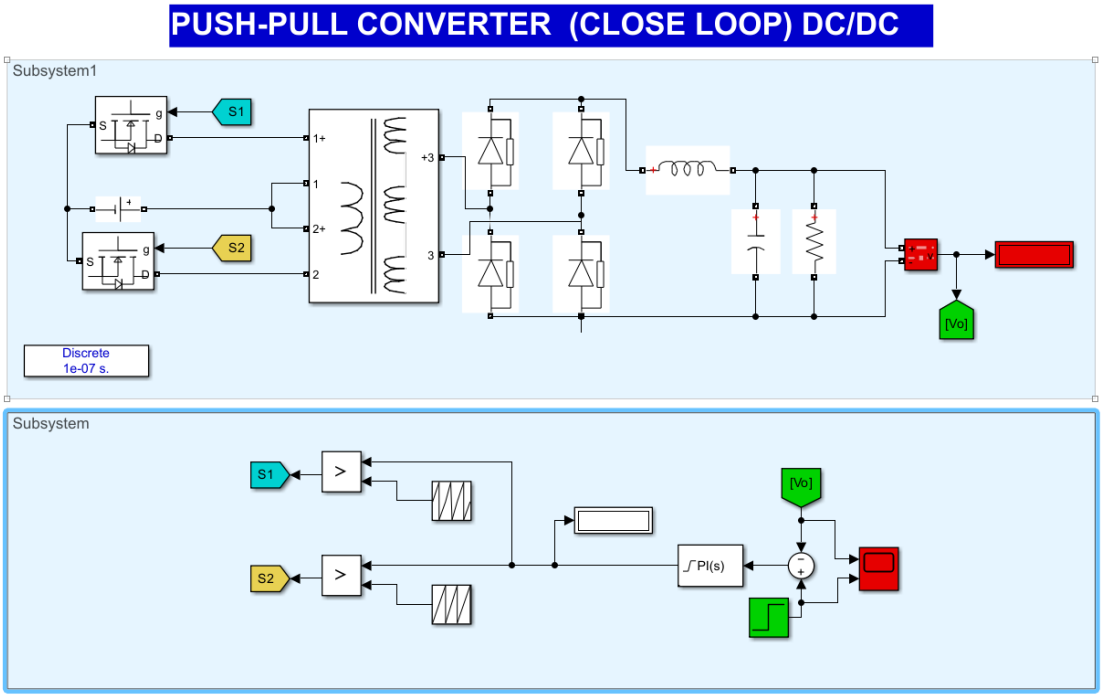

Figure 2.16: Closed loop simulations of push-pull converter with PI control .

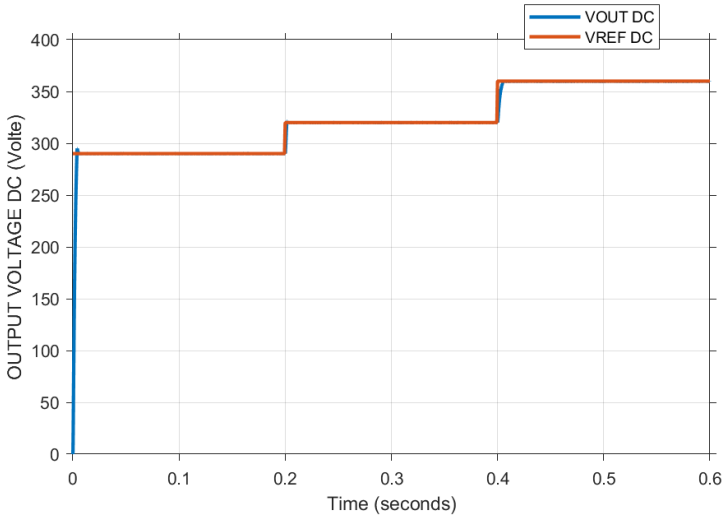

Figure 2.17: The Converter voltage with varying reference voltage .

Variable Input Voltage

In this test, we repeated the same experiment conducted in the open-loop system, as shown in Figure 2.18, and established a reference voltage of 100 V, as depicted in Figure 2.19. The results clearly demonstrate that the closed-loop system exhibits insensitivity to input voltage variations, which can be attributed to the effectiveness

of the PI controller.

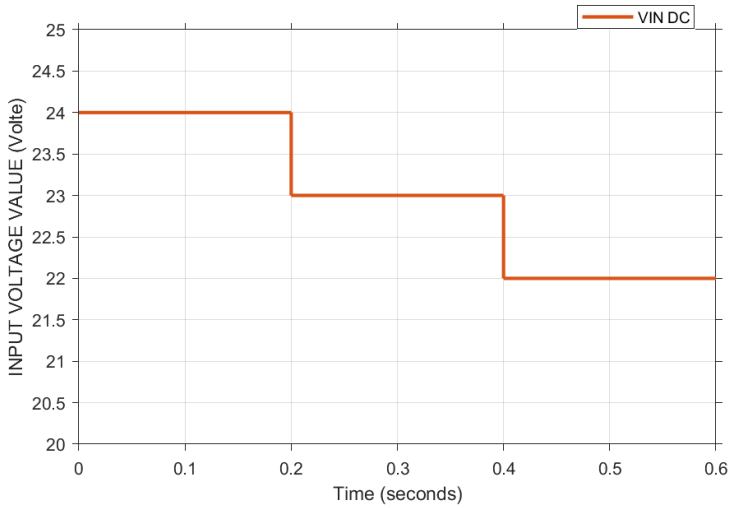

Figure 2.18: The input voltage value .

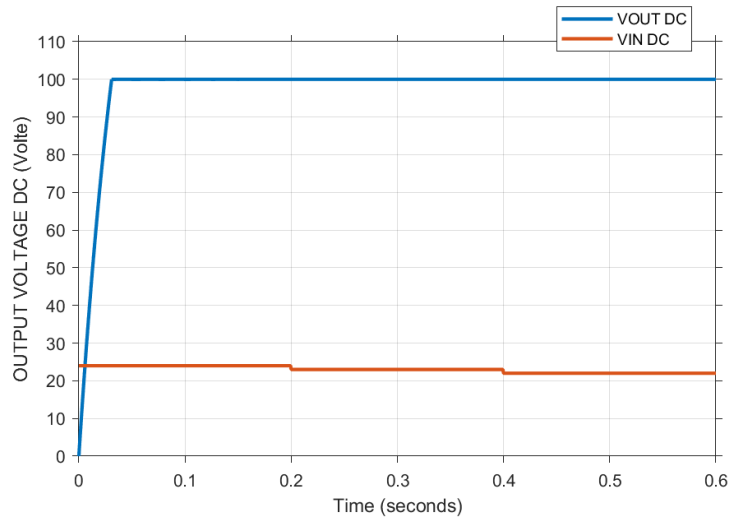

Figure 2.19: The output voltage .

Variable Load

To evaluate the robustness of the controller against load fluctuations, we set a reference voltage of 250 V while varying the resistive load from 217 Ω to 400 Ω. The results, shown in Figure 2.20, demonstrate the controller's effectiveness in quickly addressing load variations and accurately tracking the reference voltage.

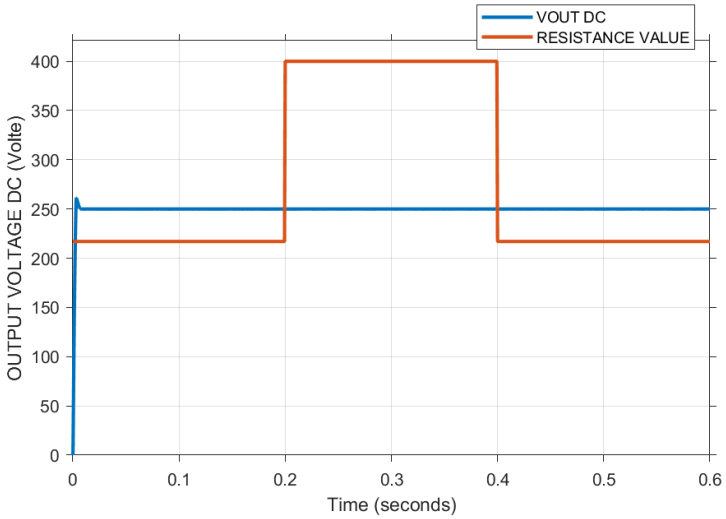

Figure 2.20: The converter's output voltage when subjected to a sudden change in load .

The results reveal significant differences between the open-loop and closed-loop configurations. In the open-loop system, we observed noticeable overshoot in the output voltage when the load is varied, whereas the closed-loop system, enhanced by the tuned PI controller, achieved stable output voltage with precise tracking of the reference voltage.

2.7 Conclusion

In summary, this chapter has explored the Push-Pull converter's topology, operation, and mathematical modeling for control purposes. We demonstrated how the Ziegler-Nichols method can be applied to design an effective PI controller for stable voltage regulation. The next chapter addresses the DC/AC stage, from modelling to control design.

3 Modelling & Control of Full Bridge Converter

3.1 Introduction

In this chapter, we provide a comprehensive understanding of the Full-Bridge converter and its operating principle, detailing its mathematical model for simulation and control using a double loop PIC controllers to achieve a good tracking of a sine wave reference voltage.

3.2 The Full-bridge converter

Figure 3.1 illustrates a DC/AC converter comprising a DC voltage source (V_{DC}), a full bridge with two legs, each containing complementary switches, an LC filter, and a load. The switches S_1 and S_2 control the full bridge, conducting when $S_i = 1$ and non-conducting when $S_i = 0$. The output voltage V_S of the full bridge depends

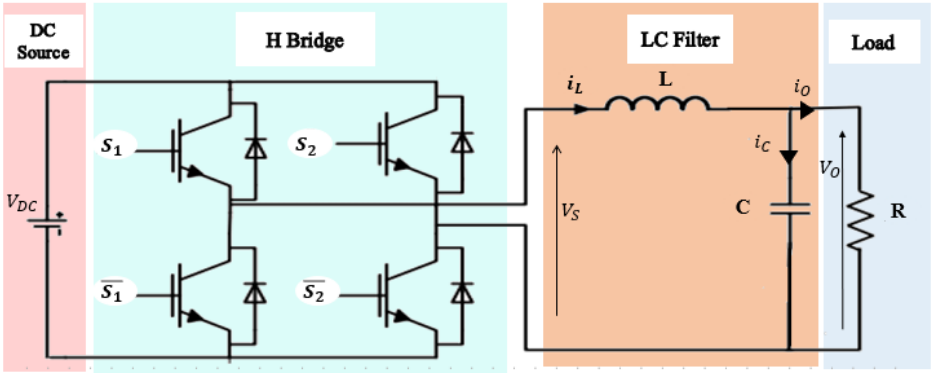

Figure 3.1: The circuit of Full-Bridge Converter.

on the switch states, resulting in three distinct voltage levels: 0, V_{DC}, and -V_{DC}. An LC filter is integrated at the full bridge output, to produce a smooth AC output voltage V_O and ensure a sinusoidal waveform under a suitable controller.

3.3 Operating Modes Of Full-Bridge Inverter

Depending one the switches states', we distinguish 4 modes:

3.3.1 Mode 1 S_1,S_4 are ON and S_2,S_3 are OFF.

In this mode, switches S_1 and S_4 are ON and S_3 and S_2 are OFF during a specific period t_1 and t_2, resulting in a positive output voltage ($V_s = +V_{dc}$) as shown in the following figure:

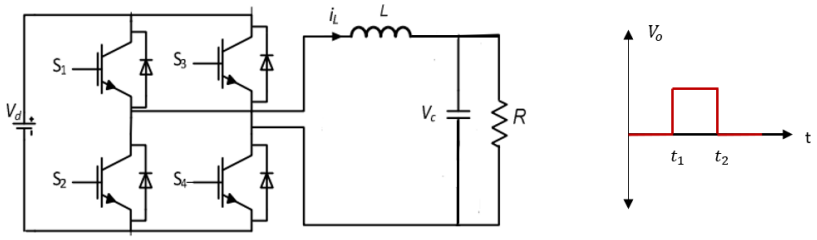

Figure 3.2: Equivalent circuit when S_1,S_4 are ON and S_2,S_3 are OFF.

3.3.2 Mode 2: S_2,S_3 are ON and S_1,S_4 are OFF.

In this case, switches S_3 and S_2 are ON while S_1 and S_4 are OFF, resulting in a negative output voltage ($V_s = -V_{dc}$) as shown below:

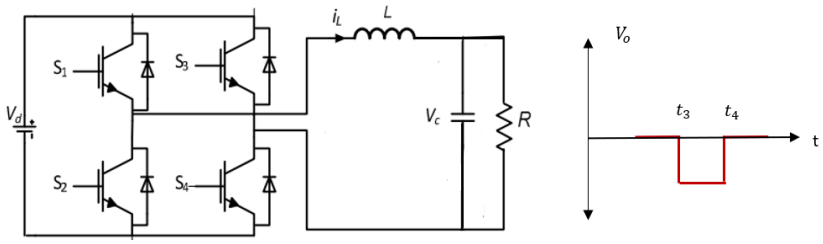

Figure 3.3: Equivalent circuit When S_2,S_3 are ON and S_1,S_4 are OFF.

3.3.3 Mode 3: S_2, S_4 are ON and S_1, S_3 OFF

In this mode, switches S_1 and S_3 are OFF, resulting in a zero output voltage ($V_s = 0$) as shown below:

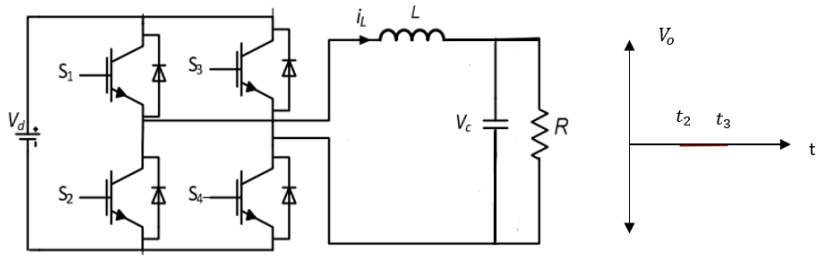

Figure 3.4: Equivalent circuit When S_2,S_4 are ON and S_1,S_3 are OFF.

3.3.4 Mode 4: S_2, S_4 are OFF and S_1, S_3 ON

This mode is similar to Mode 3 from output voltage point of view. In this case, switches S_1 and S_3 are ON, resulting in zero output voltage.

Operations Mode	S_1	S_3	Output Voltage
Mode 1	1	0	V_S = + V_{DC}
Mode 2	0	1	V_S = - V_{DC}
Mode 3	0	0	V_S = 0
Mode 4	1	1	V_S = 0

Table 3.1: Operation Modes of a Full-Bridge inverter.

3.3.5 Mathematical model

Mathematical modeling is an indispensable and important phase for dealing with physical systems in general and power converters in particular. It enables us to optimize control strategies, evaluate system performance, and ensure the stability and robustness of the system. In this section, we introduce the state-space representation of the converter and the transfer function. Prior to that, it is necessary to make the following assumptions[7]:

- Switches, diodes, capacitors, and inductors are ideal and do not have any inherent losses or non-ideal characteristics.
- The parameters of the power converter (resistance, inductance, and capacitance) remain constant over the operating range of interest.
- The switching signals applied to the power semiconductor devices are perfectly synchronized, with instantaneous transitions and no time delays.

To begin with, let's consider the LC filter model. According to Kirchhoff's current law, we have the following equation:

$$C\frac{dV_O}{dt} = i_L - i_O \tag{3.1}$$

where i_o is the output current, which is equal to $\frac{1}{R}V_O$ in the case of a resistive load.

Applying Kirchhoff's voltage law yields the following differential equation :

$$L\frac{di_L}{dt} = V_S - V_O \tag{3.2}$$

As mentioned in the previous section, the output voltage has 3 levels (V_{dc}, 0, and $-V_{dc}$) depending on the control signals S_1 and S_3. Let us consider an intermediate input signal, denoted by S, we have [7]:

- S = 1, the output voltage V_S is equal to V_{dc} and it corresponds to Mode 1.
- S = - 1, the output voltage V_S is equal to -V_{dc} and it corresponds to Mode 2.
- S = 0, the output voltage V_S is equal to 0 and it corresponds to Mode 3 and Mode 4.

Thus,equation (3.2) becomes:

$$L\frac{di_L}{dt} = V_{dc}S - V_O \tag{3.3}$$

With $S \in \{1, 0, -1\}$ is the control input, to be designed.

3.4 Average Model of the Full Bridge Inverter

3.4.1 State-Space Representation

By regrouping (3.1) and (3.3) yields to the following state-space from:

$$\begin{aligned} \dot{x} &= \mathbf{A}x + \mathbf{B}u \\ y &= \mathbf{C}x \end{aligned} \tag{3.4}$$

where

$$\mathbf{A} = \begin{bmatrix} 0 & -\frac{1}{L} \\ \frac{1}{C} & -\frac{1}{RC} \end{bmatrix}, \mathbf{B} = \begin{bmatrix} \frac{1}{L}V_{dc} \\ 0 \end{bmatrix}, \mathbf{C} = \begin{bmatrix} 0 & 1 \end{bmatrix} \tag{3.5}$$

And x $=[i_L \quad V_O]^T$ is the state variable. The next section introduces the transfer function model of the full bridge inverter.

3.4.2 Transfer Function

The average model of a DC/AC single phase inverter can be written as follows :

$$\begin{aligned} \dot{x} &= \mathbf{A}x + \mathbf{B}u \\ y &= \mathbf{C}x \end{aligned} \tag{3.6}$$

The system output corresponds to the output AC voltage V_O. Thus, the transfer function van be calculated using the following expression:

$$F(s) = \frac{Y(s)}{U(s)} = \mathbf{C}(sI - A)^{-1}B \tag{3.7}$$

Where I is the identity matrix of dimension 2. This yields to the following transfer function of the converter :

$$F(s) = \frac{V_O(s)}{U(s)} = \frac{RV_{dc}}{RLCs^2 + Ls + R} \tag{3.8}$$

3.4.3 Design of LC filter

To ensure clean power delivery to the load, a well-designed L-C filter is essential. The amount of ripple present in the inductor is influenced by its size and operating

frequency. The calculation for the filter inductance value is as follows:

$$L = \frac{V_{dc}}{4 f_s \Delta i} \tag{3.9}$$

Where V_{dc} is the input DC voltage, Δi is the amount of ripple present in the inductor current and f_s is the switching frequency.
For the allowable output voltage ripple ΔV_o, The filter capacitor can be calculated as[9]:

$$C = \frac{\Delta i}{8 f_s \Delta V_o} \tag{3.10}$$

3.5 Control System Design

3.5.1 Control Objectives

The control objectives of a full-bridge inverter is to achieve the stabilization of the AC output voltage around a sine wave reference voltage, despite any variations or disturbances in the system such as input voltage, load and converter parameters' variations. By achieving this, the inverter can effectively convert DC to AC with high precision and reliability.

3.5.2 Proposed Control Strategy

In power converters, a two-loop control system is commonly used to ensure precise and stable operation. The inner loop is responsible for current regulation, ensuring that the current follows a desired reference closely. The outer loop, on the other hand, is designed for voltage regulation. It sets the reference for the inner current loop and ensures that the output voltage remains stable and within the desired range.

In this work, we consider the commonly used two-loop control system for the full bridge inverter, where the main objective, as mentioned previously, is to force the output of the full bridge to follow a sine wave reference. Figure 3.5 illustrates the proposed control scheme for the DC/AC stage:

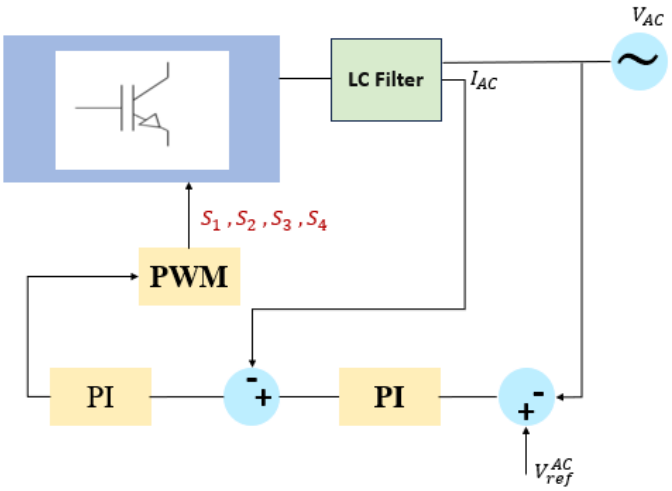

Figure 3.5: The output voltage of the close loop .

The controller parameters are designed using Ziegler-Nichols method which is summarized below (check the previous chapter for the design steps)

- First, Current control:

Type of Controller	Controller C(s)	K_p	K_i
PID	C(s) = $K_p + \frac{K_i}{s}$	$0.45K_u$	$K_i = 0.54\frac{K_u}{T_u}$

Table 3.2: The parameters of PID controller .

With : $K_p = 3.6$; $K_i = 6.4$; $K_u = 8$; $T_u = 0.675$

- Second, voltage control:

Type of Controller	Controller C(s)	K_p	K_i
PI	C(s) = $K_p + \frac{K_i}{s} + k_d$ s	$0.45K_u$	$K_i = 0.54\frac{K_u}{T_u}$

Table 3.3: The parameters of PI controller .

With : $K_p = 4.8$; $K_i = 6.4$; $K_d = 0.9$; $K_u = 8$; $T_u = 1.5$

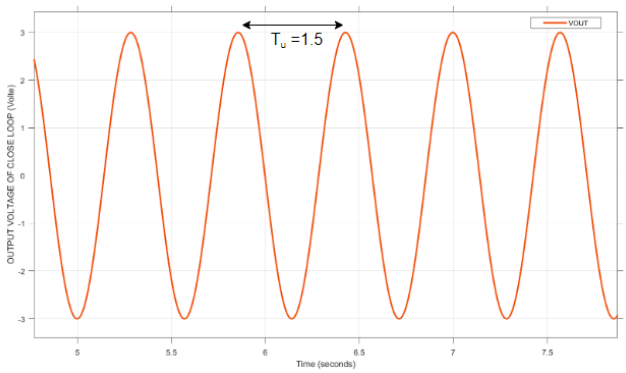

Figure 3.6: The output voltage of the converter under the outer loop control.

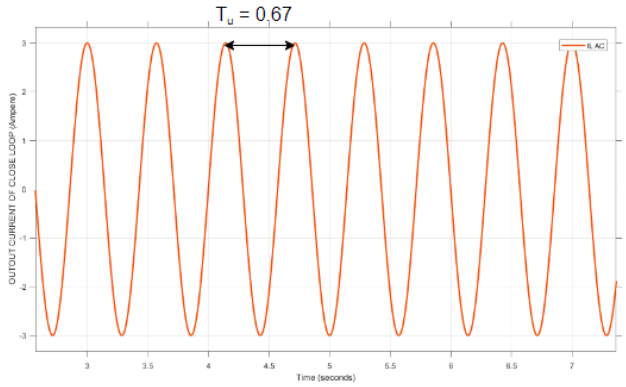

Figure 3.7: The output voltage of the converter under the inner loop control.

3.6 Simulation Results

In this part, we present the simulation results of a full bridge inverter in both open loop and closed loop configurations, using parameters obtained from an experimental setup at the LACoSERE laboratory (see Table 3.4).

Parameter	**Value**
Input voltage V_{in}	380v
Inductance (L)	0.7 mH
Capacitor (C)	26.18 µF
Load resistance (R)	1400 Ohm
Output Fundamental frequency	50Hz
Switching frequency (Fsw)	20kHZ

Table 3.4: The parameters of Full-Bridge inverter.

3.6.1 Simulation Matlab of open loop

Initially, we simulated the control of a full-bridge inverter using only PWM. This is presented as an open-loop circuit in Simulink, as shown below.

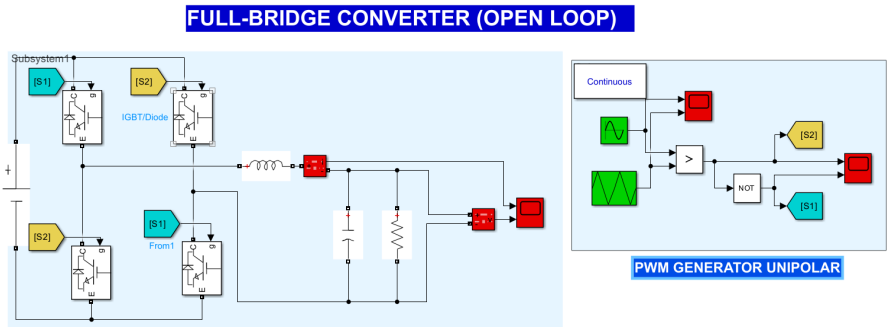

Figure 3.8: Open loop simulation of Full-Bridge inverter with PWM generator.

Test 1: Variable Input Voltage

In this section, we made changes to the input V_{in} to observe the output voltage results.

Initially, we set the input voltage V_{in} to 300V, as shown in Figure 3.9. Then, we proceeded with further variations, raising the output voltage to 380V and then to 420V. Figure 3.10 displays the results obtained, clearly demonstrating that the open-loop system exhibits sensitivity to fluctuations in the input voltage and current, as shown in Figure 3.11.

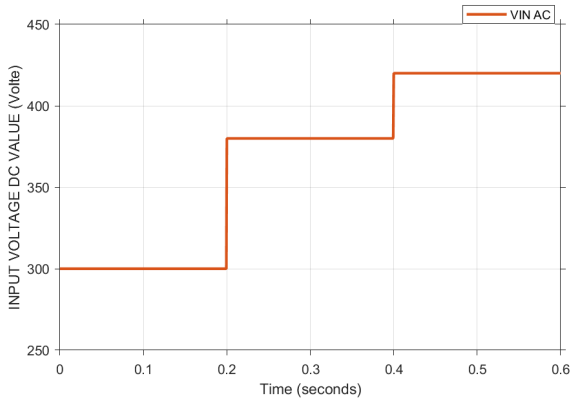

Figure 3.9: The input voltage.

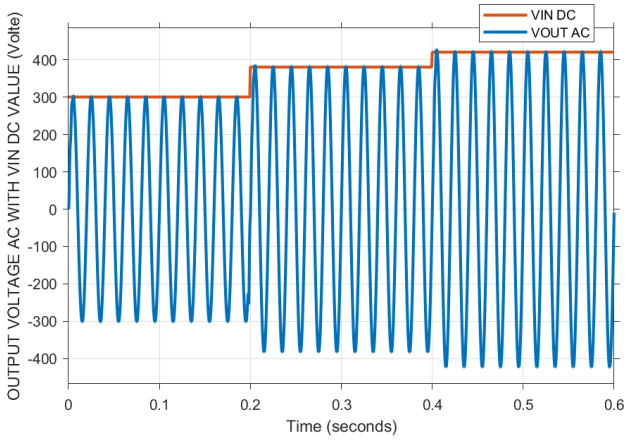

Figure 3.10: The Output voltage.

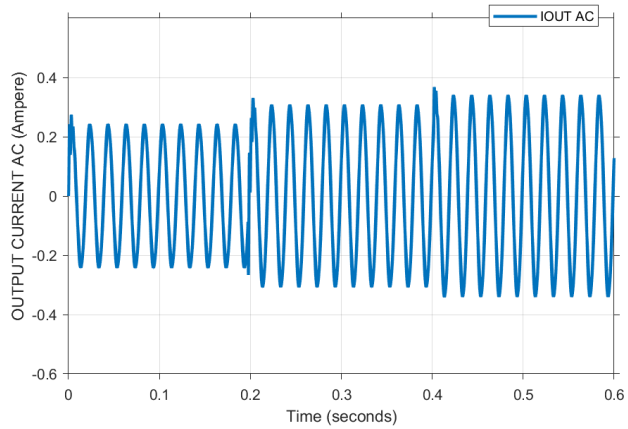

Figure 3.11: The output current .

Test 2: Variable Load

In this test, we changed the value of R_{load}, starting from 500 Ω, then increasing it to 1400 Ω, and finally to 2000 Ω to observe the effect on the output voltage with these changes.

Figure 3.13 - Figure 3.14 illustrate the evoluation of the output voltage as well as the inductor's current under these variations. We remark that output voltage keep the same amplitude and the inductor's current decreases when the load resistor increases.

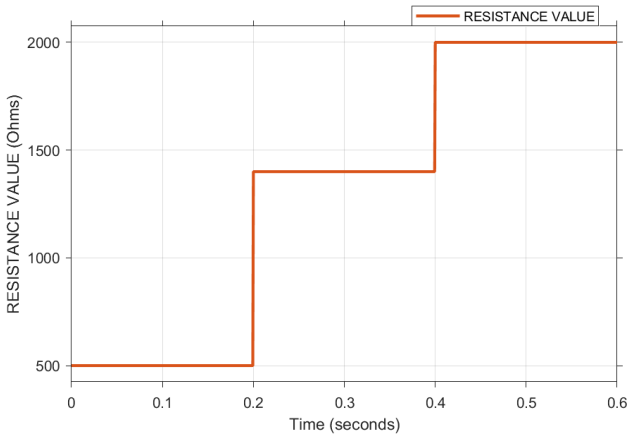

Figure 3.12: resistive load Value .

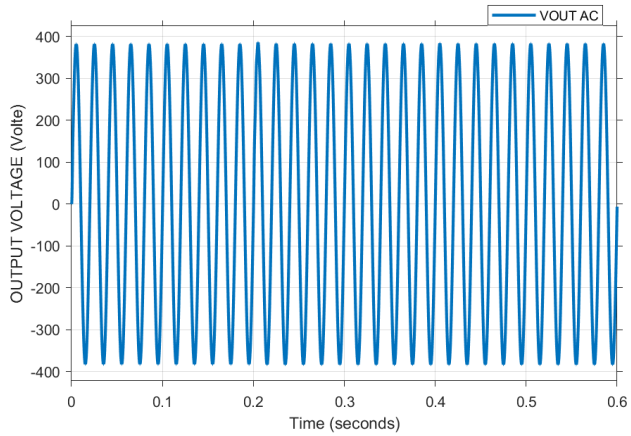

Figure 3.13: The output voltage (VOUT).

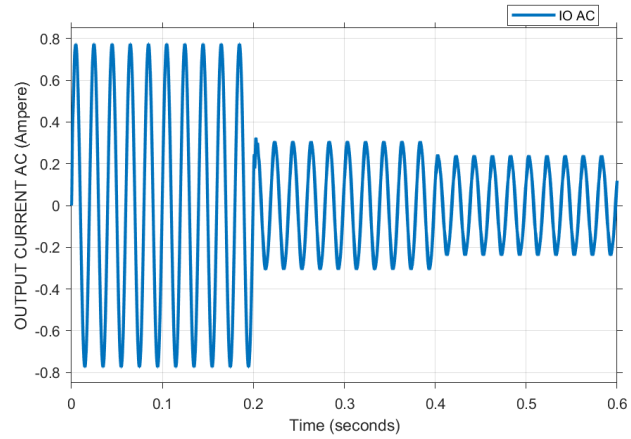

Figure 3.14: The Output current I_L evolution under variable load.

3.6.2 Simulation Matlab of Closed loop

Figure 3.15 presents the implemented full-bridge inverter in closed loop using SimScape blocks in Simulink/Matlab.

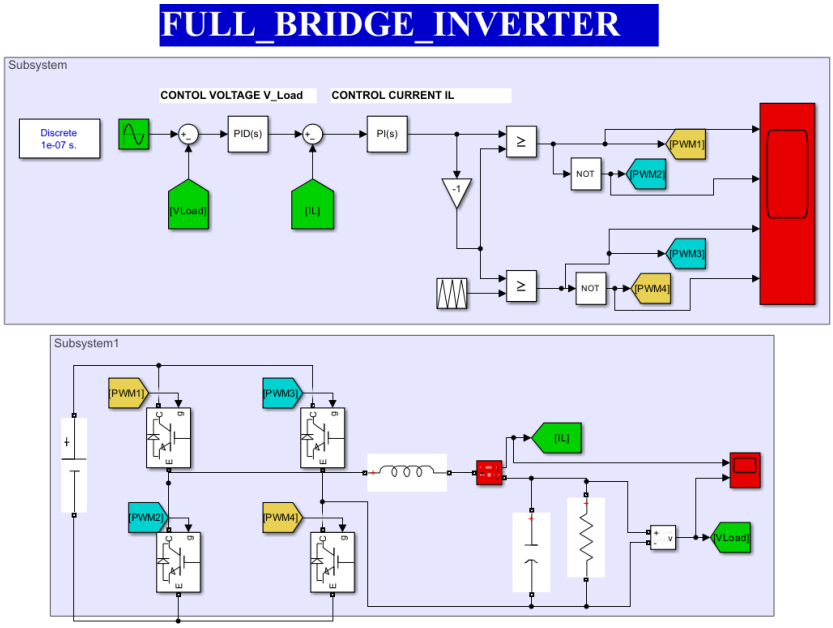

Figure 3.15: Closed loop simulation of Full-Bridge inverter.

Variable Reference Voltage

During this test, we changed the reference voltage, alternating between values of $(220\sqrt{2}\text{V})$ and $(120\sqrt{2}\text{V})$ as shown in Figures 3.16 .

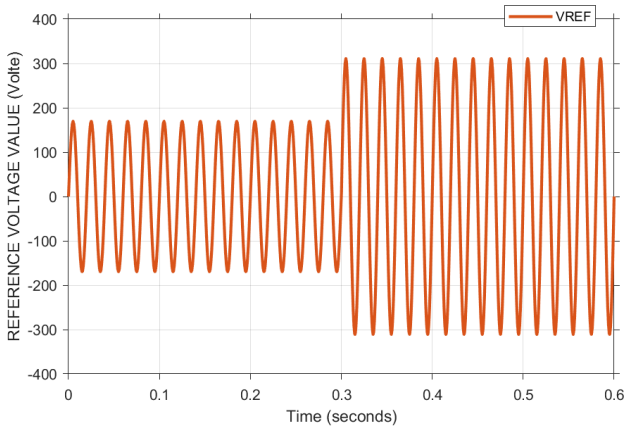

Figure 3.16: The voltage reference.

Figure 3.17 illustrates the output voltage tracking the reference voltage quickly and without any overshoot, meaning that whenever the reference voltage is changed, the output voltage promptly follows and takes on its value. Figure 3.18 represents the output current I_L for When we varied in the reference voltage :

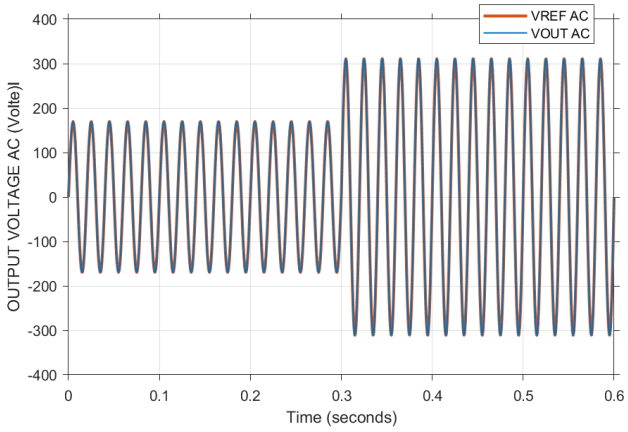

Figure 3.17: The output voltage of the converter .

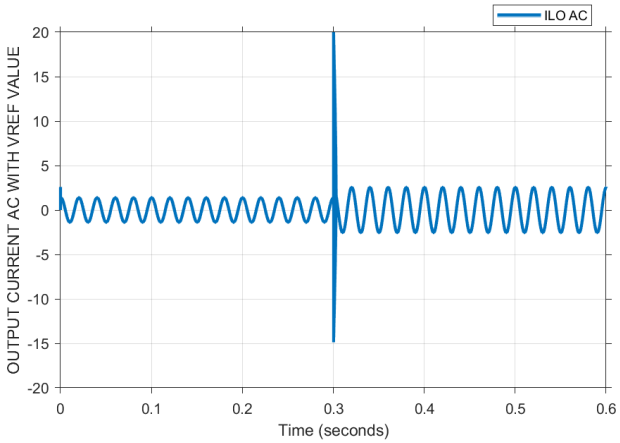

Figure 3.18: The output current I_L .

Variable Input Voltage

In this section, we made changes to the input V_{in} to observe the output voltage results. These changes included various values, starting from 300V, then increasing to 380V, and finally to 420V, as shown in Figure 3.19. Figure 3.20 displays the results obtained, clearly demonstrating that the closed-loop system shows insensitivity to variations in the input voltage, which is attributed to the two loops PI controllers. Figure3.21 represents the inductor's current current I_L.

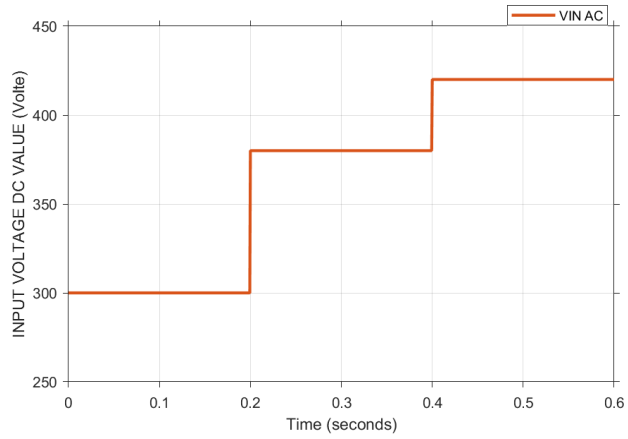

Figure 3.19: The input voltage value .

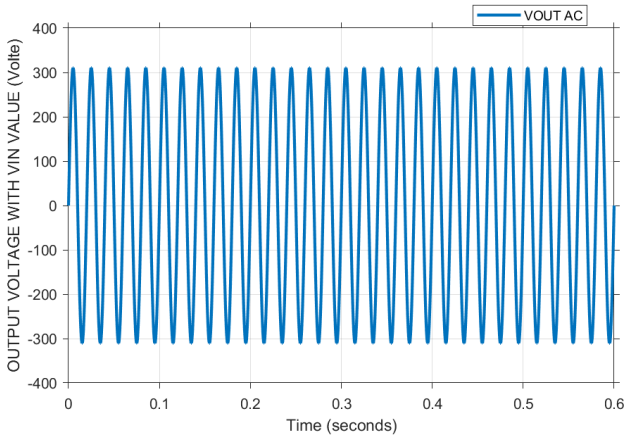

Figure 3.20: The output voltage .

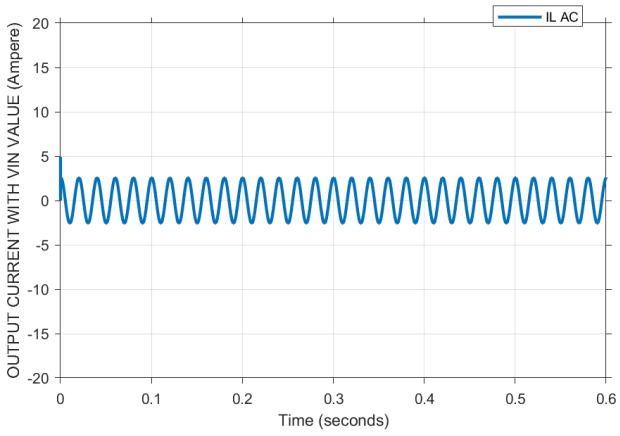

Figure 3.21: The output Current I_L .

Test 3: Variable Load

To evaluate the robustness of the controller against load variations, we varied the resistive load from 500 Ω to 1400 Ω and then to 2000 Ω, as shown in Figure 3.22.

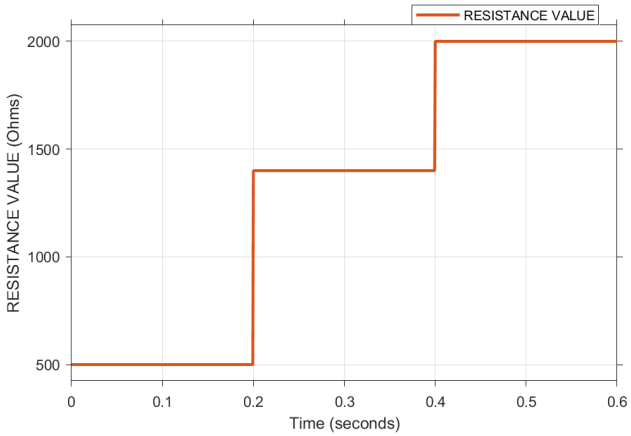

Figure 3.22: The output voltage .

The results obtained, as illustrated in Figure 3.23 and Figure 3.24, demonstrate the effectiveness of the controller in promptly addressing load variations and ensuring accurate tracking of the reference voltage.

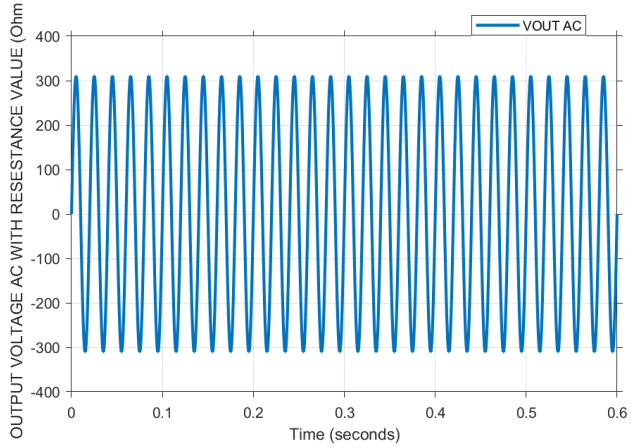

Figure 3.23: The Output Voltage .

In summary, the double-loop PI controllers for the full-bridge inverter demonstrate excellent performance in tracking the desired output voltage with minimal overshoot. The results confirm that the closed-loop system effectively maintains accurate voltage regulation despite in input voltage and load conditions.

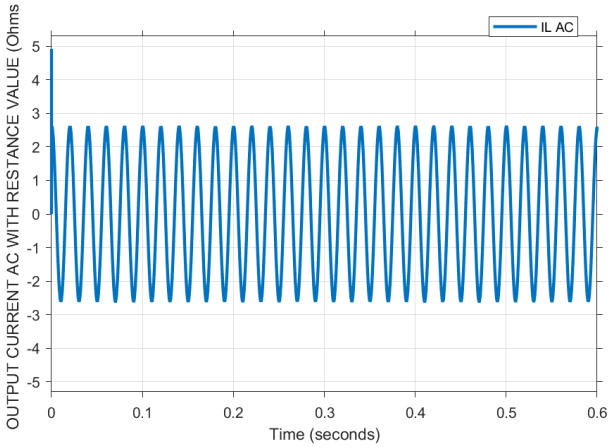

Figure 3.24: Output current I_L response .

3.7 Conclusion

In this chapter, we explored the fundamental concepts of the Full-Bridge converter, including its operating modes, mathematical model, and control strategies for sine wave generation. The state-space representation and transfer function model are provided. A double-loop PI controllers are proposed and designed using Ziegler-Nichols appraoch. Simulation results demonstrated the effectiveness of the proposed control strategy in achieving precise voltage regulation and robust performance under varying conditions. The next chapter will be devoted the association of the two power conversion stages.

4 Control of a Solar Microinverter with Soft-Start Strategy

4.1 Introduction

This chapter delves into the concept of the multistage inverter, which integrates two distinct stages of power conversion: DC/DC and DC/AC. Building on the results established in previous chapters, we explore the interaction between these two stages to achieve efficient and reliable AC voltage. The first stage, a DC/DC converter, adjusts the voltage level of its input, while the second stage, a DC/AC inverter, converts the regulated DC power into a stable AC output.

4.2 Description of the Micro-Inverter

Figure 4.1 illustrates the two stages of the micro-inverter, where each stage is defined as:

- **DC/DC Stage** : The first stage involves converting the direct current (DC) generated by solar panels into regulated direct current (DC). This is achieved using a push-pull converter, which efficiently regulates the DC voltage under various operating conditions to ensure a stable and suitable level of power for the DC-AC conversion stage. This regulation helps improve the system's efficiency and stability.

- **DC/AC Stage** : The second stage involves converting the regulated DC voltage from the first stage into AC voltage that can be used for various appli-

cations such as powering household appliances or feeding into the electrical grid. This is achieved using a DC-AC converter, also known as an inverter, specifically a full-bridge inverter. This converter enhances the system's stability and efficiency by ensuring efficient conversion of DC voltage to AC voltage while maintaining the quality and waveform of the voltage.

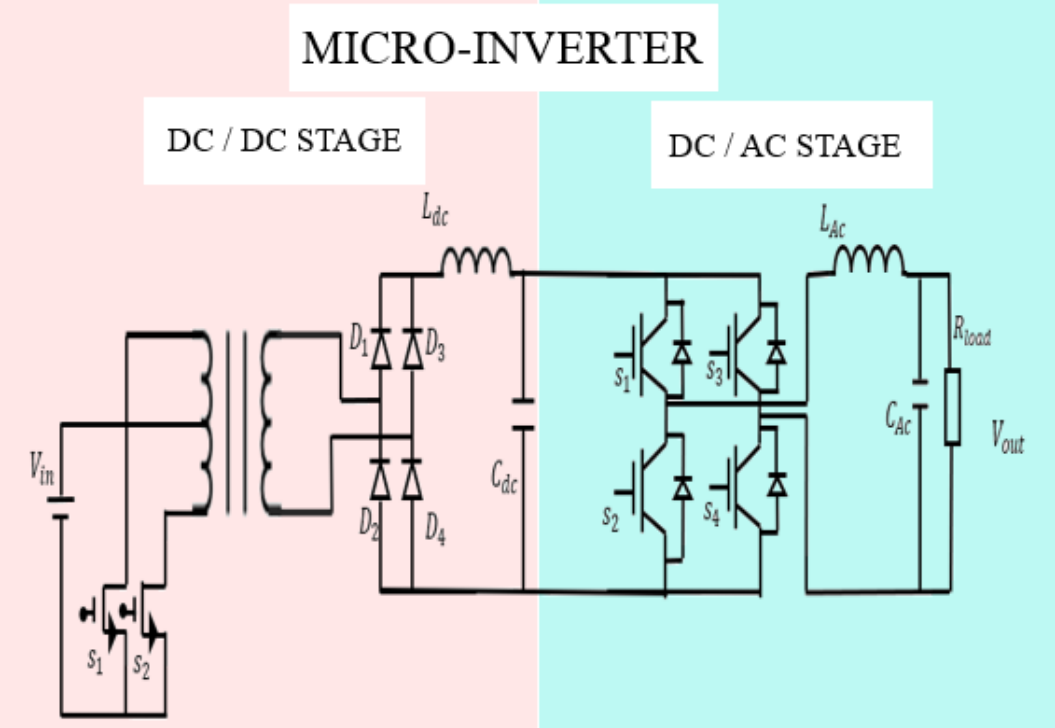

Figure 4.1: The circuit of Micro-inverter.

4.3 Mathematical model of Micro-Inverter

Since the output voltage of the push-pull converter serves as the input voltage for the single-phase inverter, the micro-inverter model is obtained by combining the models of these two stages, which were discussed in previous chapters. Let us denote :

$$\begin{gathered} x_1 = i_L^{DC}, x_2 = V_C^{DC}, x_3 = i_L^{AC}, x_4 = V_C^{AC}, \\ u_1 = d_1, u_2 = d_2 \end{gathered} \tag{4.1}$$

According to (2.10) and (3.4), the dynamics model of a solar micro-inverter is given by :

$$\begin{aligned} \dot{x_1} &= 2\frac{n}{L^{DC}}V_{in}u_1 - \frac{1}{L^{DC}}x_2 \\ \dot{x_2} &= \frac{1}{C^{DC}}x_1 - \frac{1}{C^{DC}}x_3u_2 \\ \dot{x_3} &= \frac{1}{L^{AC}}x_2u_2 - \frac{1}{L^{AC}}x_4 \\ \dot{x_4} &= \frac{1}{C^{AC}}x_3 - \frac{1}{RC^{AC}}x_4 \end{aligned} \tag{4.2}$$

Which can be written in the following from :

$$\dot{x} = f(x) + g(x)u \tag{4.3}$$

With :

$$X = \begin{bmatrix} x_1 \\ x_2 \\ x_3 \\ x_4 \end{bmatrix}; f(x) = \begin{bmatrix} -\frac{1}{L^{DC}}x_2 \\ -\frac{1}{C^{DC}}x_1 \\ -\frac{1}{L^{AC}}x_4 \\ \frac{1}{C^{AC}}x_3 - \frac{1}{RC^{AC}}x_4 \end{bmatrix}; g(x) = \begin{bmatrix} \frac{n}{L^{DC}}V_{in} & 0 \\ 0 & -\frac{1}{C^{DC}}x_3 \\ 0 & \frac{1}{L^{AC}}x_2 \\ 0 & 0 \end{bmatrix}; u = \begin{bmatrix} u_1 \\ u_2 \end{bmatrix} \tag{4.4}$$

This model is nonlinear compared to each stage of power conversion. As in this work, we consider the designed controllers in previous chapters, this model can be used to analyse the stability of the association, hence the stability of the microinverter.

4.4 Control System Design

4.4.1 Control Objectives

In multi-stage topologies of micro-solar power converters, the control objective is twofold: to maintain a stable DC bus voltage, which is the output of the push-pull converter, and to ensure that the AC output from the single-phase inverter is a clean sine wave. Achieving these objectives involves regulating the push-pull converter's output voltage around a predetermined reference and ensuring the inverter produces a stable and clean AC voltage, despite variations in load and input conditions.

4.4.2 Proposed Control diagram

The proposed control scheme for a microininverter is shown in Figure 4.2. Mainly, it consists of the association of the two closed loop systems for DC/DC stage and DC/AC stage, developed in previous chapters.

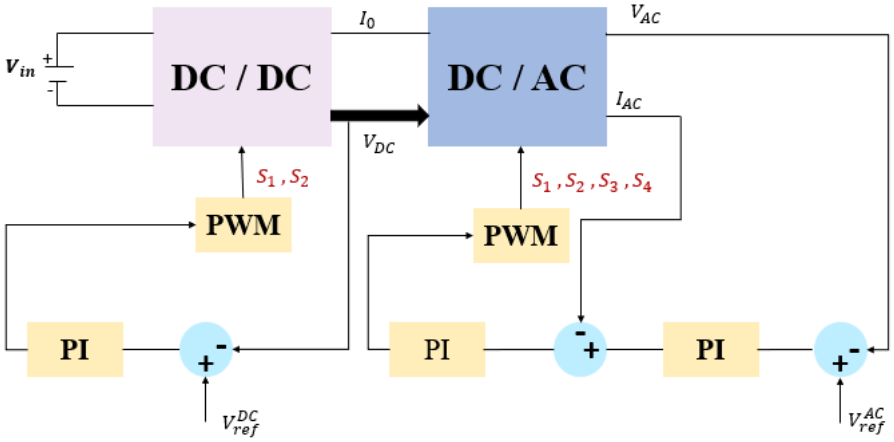

Figure 4.2: Control Design of a solar Micro-Inverter.

4.4.3 Design Methodology

The Ziegler-Nichols method is used to design the three control loops: inner current loop of the DC/AC stage for current regulation, outer loop of the DC/AC stage for AC voltage regulation, and voltage control of the DC/DC stage. Here is the steps to be followed:

- **Step 1:** Starting with the DC/AC stage and assuming constant input voltage, we implement an inner loop for current control and an outer loop for AC voltage control. Using the Ziegler-Nichols method, we design the inner loop controller. Then, we treat the DC/AC inverter with its current control scheme as a subsystem where its input is the reference current. Again, we use the Ziegler-Nichols method to design the outer loop PI controller.

- **Step 2:** The DC/AC stage and its controllers serve as a load for the DC/DC stage. Consequently, we apply the Ziegler-Nichols method to design the push-pull converter controller.

4.4.4 Soft Start Mode

The soft start mode is implemented to manage the startup process of both the DC/DC and DC/AC stages in a micro-inverter system, aiming to avoid inrush currents and ensure a smooth transition to full operation. For the DC/DC stage, this mode gradually increases the output voltage of the push-pull converter from zero to the reference value, preventing sudden surges in current and protecting system components. In the DC/AC stage, the soft start ensures that the DC input voltage reaches a sufficient level before the AC voltage is applied.

Soft Start Mode for DC/DC stage

The soft-start strategy corresponds to a reference trajectory generation. This allows a smooth transition of the output voltage of the push-pull converter from zero initial state to a reference voltage V_{ref} , as shown in the following figure:

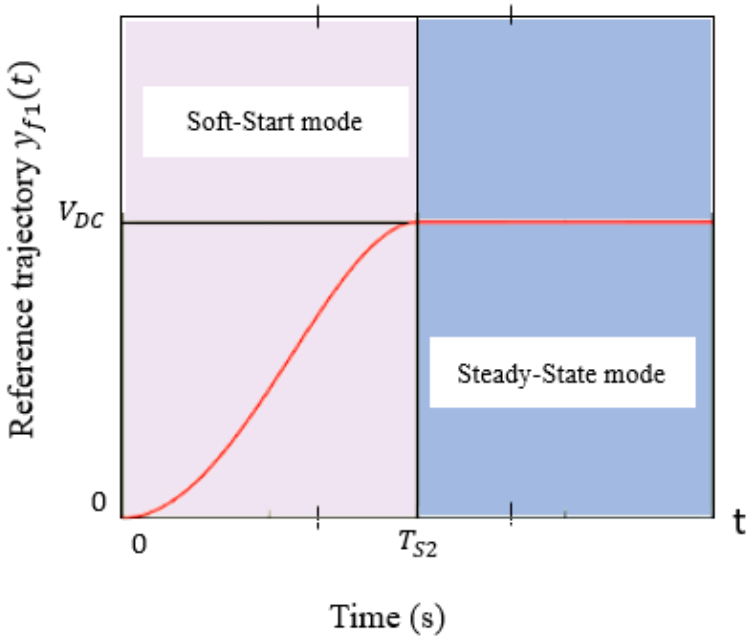

Figure 4.3: The reference voltage for DC/DC stage.

This can be achieved by a second order system as below (see Figure 4.4):

$$G(s) = \frac{K\omega^2}{s^2 + 2\xi\omega s + \omega^2} \tag{4.5}$$

With the following Parameters :

$$K = 1, \xi = 1, \omega = \frac{5.8339}{T_{s1}}$$

where T_{s1} is the settling time with a tolerance band of 2%.

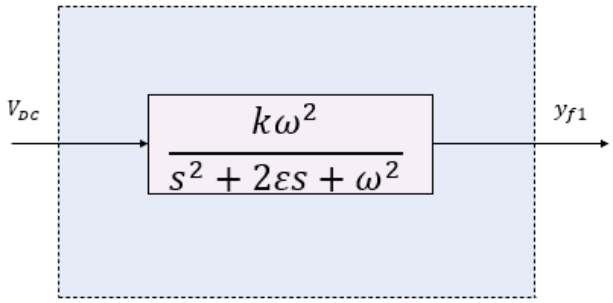

Figure 4.4: Reference trajectory generation for the DC/DC stage.

Soft Start Mode for DC/AC stage

The same idea applies for the DC/AC stage where we consider the following soft start strategy:

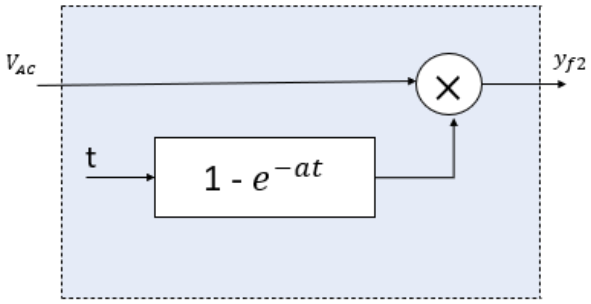

Figure 4.5: Reference trajectory generation for DC/AC stage

With : $a = \frac{\log(50)}{T_{s2}}$ and T_{s2} is the settling time with a tolerance band of 2%.

It should be noted that the soft start duration for the DC/AC stage is longer compared to the DC/DC stage ($T_{s2} > T_{s1}$). The reference AC voltage waveform is shown in the next figure:

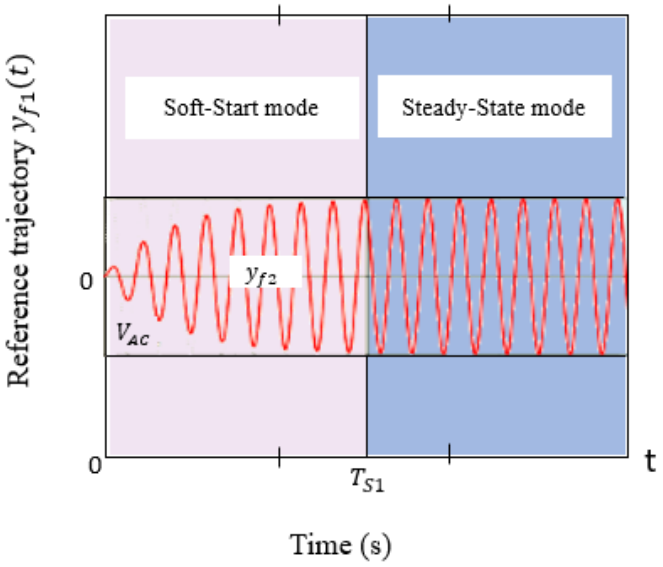

Figure 4.6: The reference voltage for DC/AC stage.

4.5 Simulation Results

In this section, **MATLAB/Simulink** was used to simulate the micro-inverter and analyze the closed loop system performance. The implemented system is shown in Figure **4.7** where parameters are reported in Chapter 2 for the DC/DC stage and chapter 3 for the DC/AC stage. Two tests are considered: variable input voltage and variable load.

4.5.1 Variable Input Voltage

Initially, we varied the input voltage V_{in} to observe its impact on the output voltages V_O^{DC} and V_O^{AC} of the converters. During the first period [0 - 0.2]s, V_{in} was set to 24 volts. It was then increased to 26 volts in the next period [0.2 - 0.4]s, and subsequently decreased to 20 volts during the final period [0.4 - 0.6]s. These variations, see Figure 4.8, were implemented to analyse the impact of V_{in} variations on the output voltages V_O^{DC} and V_O^{AC} of the converter.

We set the reference voltage V_{ref}^{DC} to 375 V, and reference voltage V_{ref}^{AC} to $220\sqrt{2}$ V. Figure 4.9 and Figure 4.10 present the evolution of the DC and AC voltages. We remark that the DC voltage tracked the reference voltage with stable fluctuations.

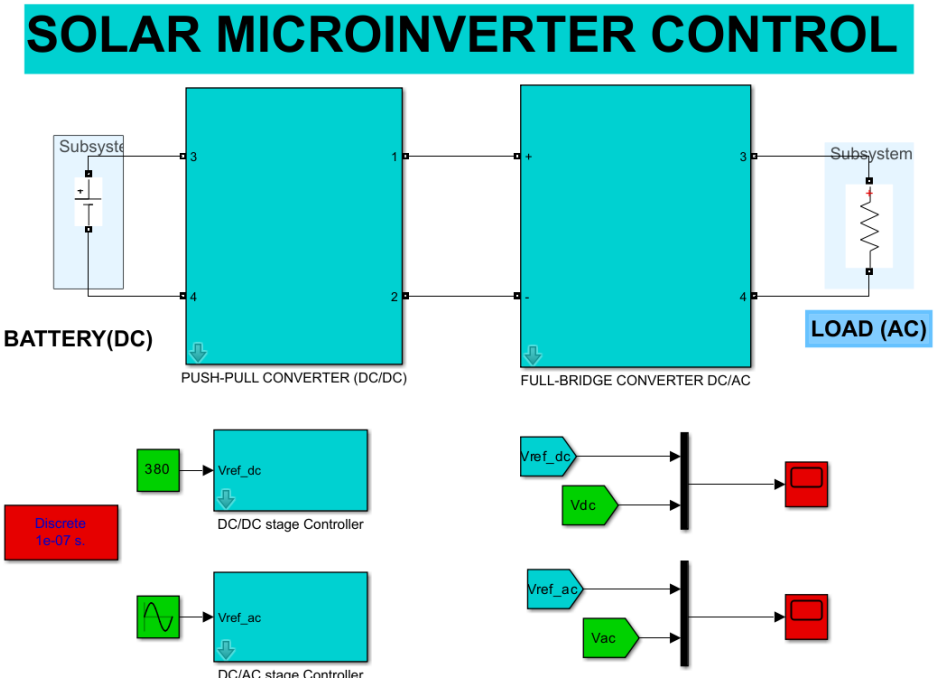

Figure 4.7: The Simulation of a solar Micro-inverter.

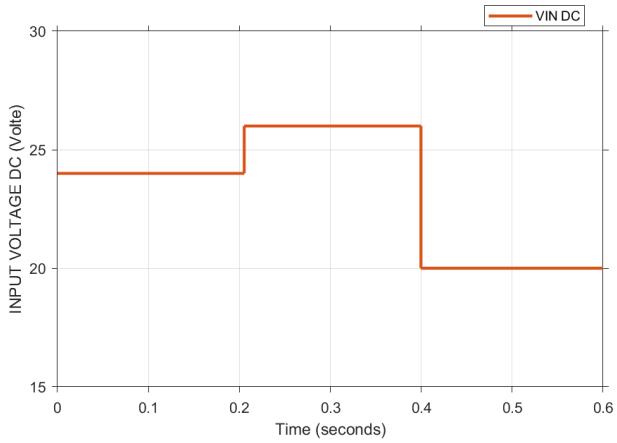

Figure 4.8: The input voltage value V_{in}.

This stabilization occurred without affecting the output voltage of the full-bridge inverter. Soft-start mode can be remarked in voltages' waveforms.

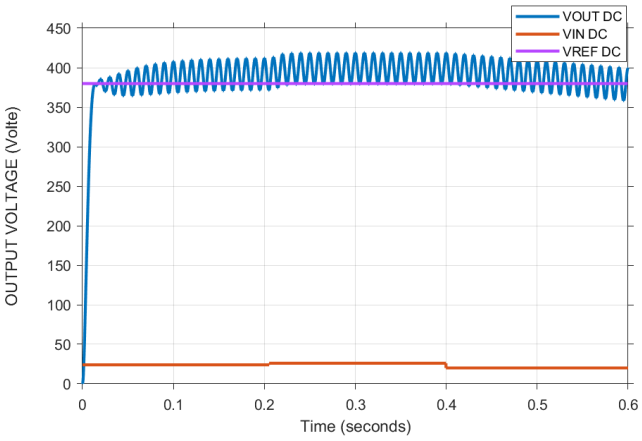

Figure 4.9: The output voltage V_{out}^{DC}.

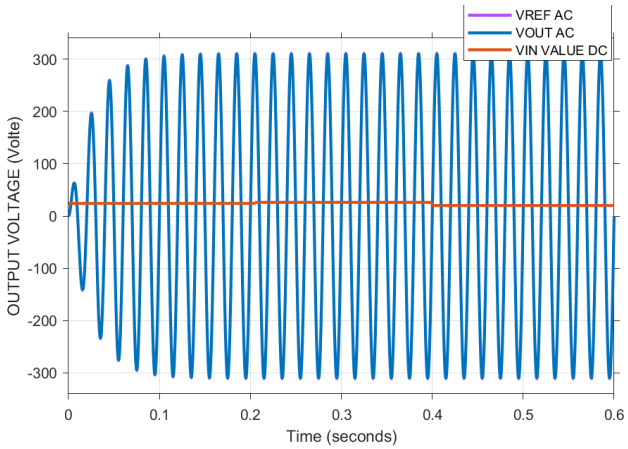

Figure 4.10: The output voltage V_{out}^{AC}.

4.5.2 Variable Load

In this test, we varied the load resistance values as follows: 500 ohms from [0 - 0.2]s, 1400 Ω from [0.2 - 0.4]s, and finally 2000 Ω from [0.4 - 0.6]s (see Figure 4.11). The reference voltage was kept constant throughout the test.

Figure 4.12 illustrates the the DC output voltage V_{DC} under load variations. The same results is remarked in the previous test, stable fluctuation that do not affect the stabilization of the AC voltage, shown in Figure 4.13.

The proposed controller for the microinverter demonstrates excellent performance in tracking the reference AC voltage and adequate performance in stabilizing the DC/DC voltage.

The presence of stable oscillations in the steady-state output of the DC/DC

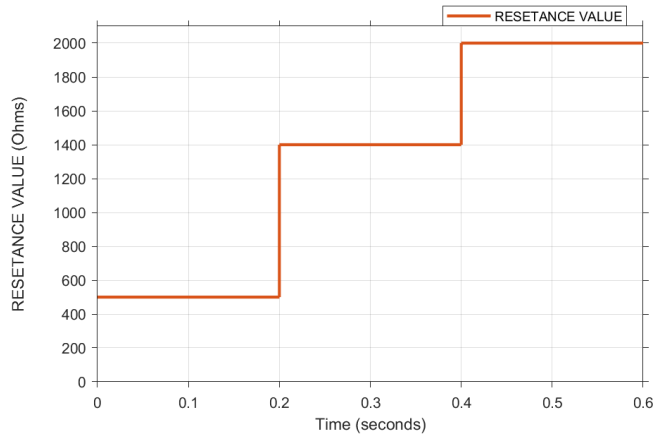

Figure 4.11: Reference Load value.

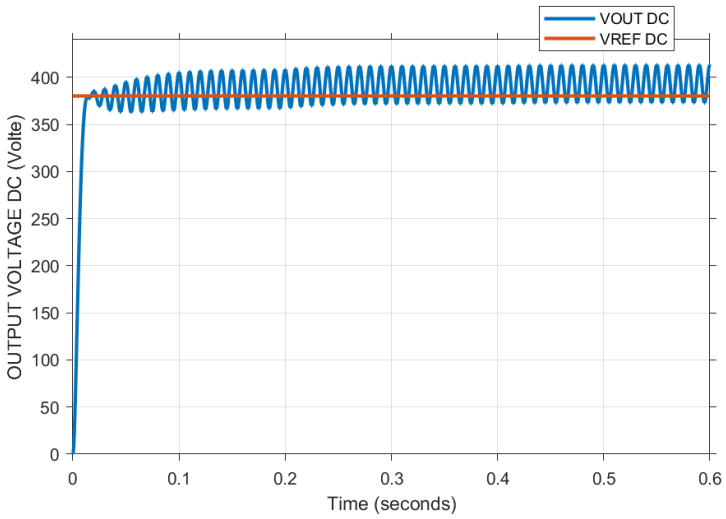

Figure 4.12: The output Voltage V_{DC}.

stage can be attributed to the decentralized nature of the control strategy, where the control of each stage operates independently without any information exchange between the DC/AC and DC/DC stages. To address this, a more advanced control strategy that integrates measurements from both stages and controls them simultaneously could be explored in future work.

4.6 Conclusion

In this chapter, we thoroughly examined the multistage inverter, which integrates two distinct power conversion stages: DC/DC and DC/AC. Through detailed

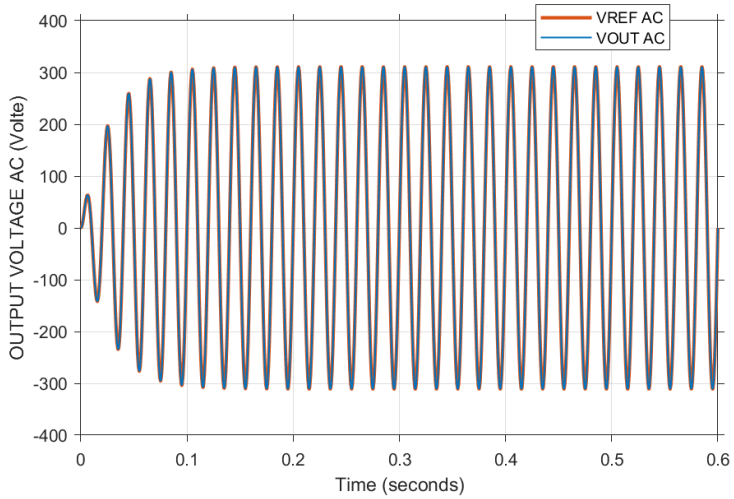

Figure 4.13: The output Voltage V_{AC}.

modeling and control design, we demonstrated the effectiveness of the proposed control strategies in achieving stable and efficient voltage regulation. The results show that the controller performs exceptionally well in tracking the reference AC voltage and reasonably well in stabilizing the DC/DC voltage, with areas for future enhancement in integrated control approaches.

General Conclusion

The work presented in this master thesis is devoted to the Modelling and Control of a solar Micro-Inverter , Primarily employed in solar inverters for both the DC-to-DC and DC-AC conversion stages, the project objectives have been effectively achieved and comprehensively outlined across the four chapters:

In Chapter One, we provided an overview of photovoltaic systems, emphasizing the crucial role of micro-inverters and their main components. We discussed the structures constituting micro-inverters, including both isolated and non-isolated DC-DC converters, and DC-AC converters, and highlighted the chosen topology for this project.

Chapter Two delved into the push-pull converter's topology, operation, and mathematical modeling for control purposes. We applied the Ziegler-Nichols method to design a PI controller for stable DC voltage regulation.

In Chapter Three, we explored the fundamental concepts of the full-bridge converter, including its operating modes, mathematical model, and control strategy for sine wave generation. We designed double-loop PI controllers with the Ziegler-Nichols approach. Simulation results validated the effectiveness of the control strategy in achieving precise voltage regulation and robust performance under varying conditions.

Chapter Four integrated the two power conversion stages, DC-DC and DC-AC, demonstrating the effectiveness of the proposed control strategies in achieving stable and efficient voltage regulation. While the controller showed excellent

performance in tracking the reference AC voltage and reasonable performance in stabilizing the DC-DC voltage, we identified areas for improvement.

The presence of stable oscillations in the DC-DC stage's steady-state output highlighted the need for a more advanced control strategy that integrates measurements from both stages and controls them simultaneously. To enhance the obtained results about controlling solar micro-inverters, several areas for development and improvement can be proposed:

- **Advanced Nonlinear Control Strategies**: Develop and implement advanced nonlinear control strategies that incorporate system states to define the control of both the DC-DC and DC-AC stages. This approach could help achieve better stability and performance by considering the interactions between the stages.

- **Integration and Testing with Complete Systems**: Integrate the solar micro-inverter with photovoltaic panels, batteries, and loads to test its performance in a real-world scenario. This integration would provide insights into the practical challenges and effectiveness of the proposed control strategies in a complete PV system.

- **Experimental Implementation**: Conduct an experimental implementation of the proposed control strategies on a solar micro-inverter. This practical validation would demonstrate the feasibility and robustness of the control approaches, providing valuable feedback for further refinements and optimizations.

Bibliography

[1] M Serge POIGNANT. Rapport d'information.

[2] Soeren Baekhoej Kjaer, John K Pedersen, and Frede Blaabjerg. Power inverter topologies for photovoltaic modules-a review. In Conference Record of the 2002 IEEE Industry Applications Conference. 37th IAS Annual Meeting (Cat. No. 02CH37344), volume 2, pages 782–788. IEEE, 2002.

[3] Soeren Baekhoej Kjaer, John K Pedersen, and Frede Blaabjerg. A review of single-phase grid-connected inverters for photovoltaic modules. IEEE transactions on industry applications, 41(5):1292–1306, 2005.

[4] Yi-Hung Liao and Ching-Ming Lai. Newly-constructed simplified single-phase multistring multilevel inverter topology for distributed energy resources. IEEE Transactions on Power Electronics, 26(9):2386–2392, 2011.

[5] M LokeshReddy, PJR Pavan Kumar, S Aneel Manik Chandra, T Sudhakar Babu, and N Rajasekar. Comparative study on charge controller techniques for solar pv system. Energy Procedia, 117:1070–1077, 2017.

[6] Wilson CP De Aragao Filho and Ivo Barbi. A comparison between two current-fed push-pull dc-dc converters-analysis, design and experimentation. In Proceedings of Intelec'96-International Telecommunications Energy Conference, pages 313–320. IEEE, 1996.

[7] N.Abouchabana A.Hadjaissa A.Benalia M.benmiloud, K.Ameur. Proportional resonant controller design with anti-windup for a single phase inverter. Submitted to Renewable and Sustainable Energy Reviews, 67:1065–1080, 2024.

[8] SMRITI YADAV and VIJAY BHURIA. Tuning of pid controller using zeigler nichols and particle swarm optimization in avr system. 2015.

[9] Praveen Kumar Bonthagorla and Suresh Mikkili. Performance analysis of closed loop controlled single-phase unipolar inverter with fixed switching frequency sliding mode control. In 2019 IEEE 1st International Conference on Energy, Systems and Information Processing (ICESIP), pages 1–6. IEEE, 2019.